

# Biological evaluation of lanthanide-based near-infrared imaging agents for the specific recognition of HER2 protein in a breast cancer model

---

Ćutuk, Petra

Master's thesis / Diplomski rad

2023

Degree Grantor / Ustanova koja je dodijelila akademski / stručni stupanj: **University of Zagreb, Faculty of Food Technology and Biotechnology / Sveučilište u Zagrebu, Prehrambeno-biotehnološki fakultet**

Permanent link / Trajna poveznica: <https://urn.nsk.hr/urn:nbn:hr:159:426569>

Rights / Prava: [Attribution-NonCommercial-NoDerivs 3.0 Unported / Imenovanje-Nekomercijalno-Bez prerađivanja 3.0](#)

Download date / Datum preuzimanja: **2024-06-30**



Repository / Repozitorij:

[Repository of the Faculty of Food Technology and Biotechnology](#)



Sveučilište u Zagrebu  
Prehrambeno – biotehnološki fakultet  
Molekularna biotehnologija

Diplomski rad

**Biolška procjena agenasa temeljenih na lantanidima u bliskom  
infracrvenom području za specifično prepoznavanje HER2 proteina  
u modelu raka dojke**

Petra Ćutuk, 0217 MB

Institut i adresa: Centar za molekularnu biofiziku, Rue Charles Sadron, CNRS UPR4301, 45071  
Orléans, Francuska

Tim: Luminescentni lantanoidni spojevi, optička spektroskopija i bioimaging

Mentor: Dr. Julie Bourseguin i Dr. Marie-Aude Hiebel

Voditelj tima: Dr. Proff. Stéphane Petoud

Zagreb, lipanj 2023.

University of Zagreb  
Faculty of Food Technology and Biotechnology  
Molecular biotechnology

Master thesis

**Biological evaluation of lanthanide-based near-infrared imaging  
agents for the specific recognition of HER2 protein in a breast  
cancer model**

Petra Ćutuk, 0217 MB

Internship institution and address: Centre for Molecular Biophysics, Rue Charles Sadron,  
CNRS UPR4301, 45071 Orléans, France

Team: Luminescent lanthanide compounds, optical spectroscopy and bioimaging

Mentor: Julie Bourseguin, Associate Professor, PhD and Marie-Aude Hiebel, Associate  
Professor PhD

Group leader: Stéphane Petoud, Professor, PhD

Zagreb, June 2023.



## Université d'Orléans-Université de Zagreb

UFR Sciences et Techniques - Faculté de Nutrition et Biotechnologie - Faculté des Sciences

### MASTER SCIENCES DU VIVANT

Spécialité : **Techniques Bio-Industrielles**

INTERNSHIP REPORT

## Biological evaluation of lanthanide-based near-infrared imaging agents for the specific recognition of HER2 protein in a breast cancer model

By

Petra Ćutuk

(February 2023 – June 2023)

**Internship institution and address:** CNRS – Center for Molecular Biophysics (CBM),  
Rue Charles Sadron, 45071 Orléans, France

**Mentors:** Julie Bourseguin, Associate Professor, PhD and Marie-Aude Hiebel, Associate Professor PhD

**Supervisor:** Stéphane Petoud, Professor, PhD



## Acknowledgments

I would like to express my deepest gratitude to my mentors *Dr. Julie Bourseguin* and *Dr. Marie-Aude Hiebel* for showing me their trust and giving me the opportunity to work on this project for my master's thesis. Their insight and knowledge of the subject matter steered me through this project, and I am extremely grateful for their patient guidance and their help and valuable advice throughout the project; from planning the project, performing the experiments, discussing results to immense help in writing thesis. Thank you for all answered questions and the perfect balance between supervision and independence. I hope that I justified your belief in my work.

I would like to express my deep appreciation to my supervisor *Professor Stéphane Petoud* for the knowledge he passed on to me, for all the help during my internship and for really making me feel as a part of the team.

I would like to extend my thanks to *Dr. Svetlana Eliseeva* for all the advice, the transferred knowledge and the helpful suggestions during my internship.

Many thanks to the coordinators of my study program; Professor Josef Hamacek, Professor Chantal Pichon, Professor Igor Stuparević, Professor Vladimir Mrša and Professor Višnja Besendorfer for all their hard work in organizing and conducting the study program between Zagreb and Orléans that enabled me to come to France and do my thesis there.

Special thanks to my friends and colleagues, whose support and encouragement helped me overcome challenges and who made my stay in France unforgettable.

I would also like to thank my dear colleague *Codruța Bădescu* for being great colleague, for all the invitations and for filling me in on all the details of the team work.

Most sincere gratitude goes to my family – my parents *Monika* and *Željko*, my sisters *Patricia* and *Anđela*, my brother *Petar*, my best friends: *Kika*, *Ante*, *Roko*, *Iva*, *Marija Terezija* and *Ivana*. Thank you for the enormous amount of support and love you have always given me. Thank you for always believing in me.

And finally, I owe my greatest gratitude to dear God for guidance, protection and all the blessings and graces.

## TEMELJNA DOKUMENTACIJSKA KARTICA

Diplomski rad

Sveučilište u Zagrebu

Prehrambeno-biotehnološki fakultet

Centar za molekularnu biofiziku, CNRS, Orléans, Francuska

Znanstveno područje: Biotehničke znanosti

Znanstveno polje: Biotehnologija

### Biološka procjena agenasa temeljenih na lantanidima u bliskom infracrvenom području za specifično prepoznavanje HER2 proteina u modelu raka dojke

Petra Ćutuk, 0058214615

**Sažetak:** Rak dojke (BC) jedna je od najčešćih zloćudnih bolesti u svijetu i vodeći uzrok smrti kod žena. HER2 pozitivan rak dojke (prekomjerna ekspresija HER2 receptora) predstavlja vrlo agresivan podtip i čini 15-20% slučajeva raka dojke. U ovom diplomskom radu se izvještava o razvoju dijagnostičkog alata temeljenog na polistirenskim kuglicama koje sadrže „metallacrowns“ na bazi lantanida na koje je vezan trastuzumab (Trz) u reakciji biološke konjugacije. Dobivene anti-HER2 konjugirane kuglice testirane su *in vitro* u studijama afiniteta, citotoksičnosti i proliferacije. Konjugirani spoj pokazao je očuvani afinitet vezanja za HER2 protein i specifične interakcije sa stanicama s prekomjernom ekspresijom HER2, bez značajnijeg citotoksičnog učinka dok inhibira proliferaciju stanica s prekomjernom ekspresijom HER2 receptora. Ovi nalazi sugeriraju potencijal Trz-kuglica kao ciljanog dijagnostičkog alata za HER2-pozitivan rak dojke.

**Glavne riječi:** rak dojke, HER2 receptor, biokonjugacija, polistirenske kuglice, „metallacrowns“, trastuzumab, lantanidi, blisko infracrveno područje, nanotehnologija.

**Rad sadrži:** 30 stranica, 17 slika, 1 tablicu, 47 literaturnih navoda

**Jezik izvornika:** engleski

**Rad je u tiskanom i elektroničkom obliku pohranjen u:** knjižnici Prehrambeno-biotehnološkog fakulteta Sveučilišta u Zagrebu, Kačićeva 23, 10 000 Zagreb

**Mentor:** Dr. Julie Bourseguin i Dr. Marie-Aude Hiebel

**Voditelj tima:** Dr. Proff. Stéphane Petoud

**Stručno povjerenstvo za ocjenu i obranu:**

1. Prof. dr. sc. Igor Stuparević
2. Prof. dr. sc. Višnja Besendorfer
3. Prof. dr. sc. Katel Hervé Aubert
4. Doc. dr. sc. Bojan Žunar
5. Prof. dr. sc. Julie Bourseguin
6. Prof. dr. sc. Josef Hamaček
7. Prof. dr. sc. Chantal Pichon

**Datum obrane:** 3. srpnja 2023.

## BASIC DOCUMENTATION CARD

Master thesis

**University of Zagreb**

**Faculty of Food technology and Biotechnology**

**Centre for Molecular Biophysics, CNRS, Orléans, France**

**Scientific area:** Biotechnical Sciences

**Scientific field:** Biotechnology

### **Biological evaluation of lanthanide-based near-infrared imaging agents for the specific recognition of HER2 protein in a breast cancer model**

Petra Ćutuk, 0217 MB

**Abstract:** Breast cancer (BC) is one of the most common malignancies worldwide and a leading cause of death among women. The HER2 positive breast cancer (overexpressing HER2 receptor) represents a very aggressive subtype and constitutes 15-20% of BC cases. Here we report about the creation of new diagnostic tool based on polystyrene beads incorporating Ln-based metallacrowns that were biologically targeted in a reaction of conjugation with Trastuzumab (Trz). The bioconjugation reaction was performed under various conditions. The resulting anti-HER2 conjugated beads were tested *in vitro* in studies of affinity, cytotoxicity and proliferation. We managed to do successful bioconjugation of Trz to polystyrene beads under optimized conditions. The conjugated compound exhibited preserved binding affinity for HER2 and showed specific interactions with HER2-overexpressing cells, the conjugate did not display extensive cytotoxic effects but inhibited the proliferation of HER2-overexpressing cells. These findings suggest the potential of Trz-beads as a targeted diagnostic tool for HER2-positive breast cancer.

**Key words:** breast cancer, HER2 receptor, bioconjugation, polystyrene beads, metallacrown, Trastuzumab, lanthanide, near-infrared, nanotechnology.

**Thesis contains:** 30 pages, 17 Figures, 1 Table, 47 references

**Original in:** English

**Master thesis in printed and electronic version deposited in:** Library of the Faculty of Food technology and Biotechnology, Kačićeva 23, 10 000 Zagreb

**Mentor:** Julie Bourseguin, Associate Professor, PhD and Marie-Aude Hiebel, Associate Professor PhD

**Group leader:** Stéphane Petoud, Professor, PhD

**Reviewers:**

1. Prof. dr. sc. Igor Stuparević
2. Prof. dr. sc. Višnja Besendorfer
3. Prof. dr. sc. Katel Hervé Aubert
4. Doc. dr. sc. Bojan Žunar
5. Prof. dr. sc. Julie Bourseguin
6. Prof. dr. sc. Josef Hamaček
7. Prof. dr. sc. Chantal Pichon

**Thesis defended:** June 3<sup>rd</sup> 2023.

## **Presentation of the Laboratory and localization of the internship**

The Center for Molecular Biophysics (CBM) is a research unit of the French National Center for Scientific Research (Centre National de la Recherche Scientifique, CNRS), affiliated with the University of Orléans. Since January 2022, CBM is headed by Dr Matthieu Réfrégiers. CBM research is organized around four scientific departments and a research support service. A multidisciplinary research center focuses on the understanding the fundamental principles of life at the molecular level. Established in 1967, CBM is based on interdisciplinary collaborations between biologists, chemists and physicists. Research focuses on the investigation of the structure, dynamics, and interactions of biomacromolecules at the molecular, cellular and organism level.

My traineeship was performed in the “Luminescent lanthanide compounds and, optical spectroscopy and bioimaging” research group, led by Professor Stéphane Petoud. The current main research interest of the group is the creation of innovative molecular systems with unique luminescent properties and applications in various fields, including biological imaging, sensing and diagnostics. Additionally, Professor Petoud’s group is working on the design and synthesis of coordination compounds, such as lanthanide complexes, which can be used as molecular probes to investigate biological phenomena, including metal ion interactions, enzyme activity, cellular processes, as well as developing fluorescent-based imaging agent specific of a targeted tissue.

# Table of content

INTERNSHIP REPORT .....	3
1. INTRODUCTION.....	1
1.1 Breast cancer .....	1
1.1.1. HER2-positive breast cancer.....	2
1.1.2. Targeted therapy for the treatment of HER2+ breast cancer: focus on Trastuzumab.....	4
1.2. Near infrared imaging.....	5
1.2.1. Fluorescence properties and advantages in biological conditions.....	5
1.2.2. Development of fluorescence guided surgery .....	6
1.2.3. Luminescent lanthanide: Advantages and Challenges.....	8
1.7. Objective.....	10
2. MATERIALS AND METHODS.....	12
2.1. Cell lines.....	12
2.2. Bioconjugation of Trastuzumab and polystyrene beads .....	12
2.3. Synthesis of the Zn <sup>16</sup> Yb(quinHA) <sub>16</sub> metallacrown and incorporation in polystyrene beads..	13
2.4. Concentration of coupled antibodies.....	13
2.5. Enzyme-linked immunosorbent assay (ELISA) .....	14
2.6. Cytotoxicity assay .....	14
2.7. Cell proliferation assay .....	15
2.8. Western blot .....	15
2.10. NIR epifluorescence microscopy.....	16
3. RESULTS.....	18
3.1. Choice of cell lines.....	18
3.2. Antibodies reduction and bioconjugation .....	18
3.3. ELISA .....	20
3.4. Cell viability.....	21
3.5. Cell proliferation .....	22
3.6. HER2 expression.....	23
3.7. Spectroscopic characterization of the conjugated beads containing the NIR emitting metallacrown.....	24
3.8. NIR epifluorescence microscopy.....	25
4. DISCUSSION AND CONCLUSIONS.....	27
5. REFERENCES.....	31

## List of abbreviations

BC breast cancer

HER human epidermal growth factor receptor

ERBB/EGFR epidermal growth factor receptor

PI3K/Akt phosphatidylinositol 3-kinase/protein kinase B

MAPK / ERK1/2 mitogen-activated protein kinase / extracellular-related kinase ½

ECD extracellular ligand-binding domain

FDA Food and Drug Administration

IHC immunohistochemistry

FISH fluorescence *in situ* hybridization

ASCO American Society of Clinical Oncology

CAP College of American Pathologists

CISH chromogenic *in situ* hybridization

SISH silver-enhanced *in situ* hybridization

ADCC antibody-dependent cell-mediated cytotoxicity

MC metallacrown

NIR near infrared

CT computed tomography

MRI magnetic resonance imaging

Trz Trastuzumab

BTC betacellulin

EPG epigen

EPR epiregulin

HB-EFG heparin-binding EGF-like ligand

NRG neuregulin

Trz-Beads Trastuzumab-coupled beads

Trz-Ln-Beads Trastuzumab-coupled lanthanide-based beads

DMEM Dulbecco's modified Eagle medium

BCA assay bicinchoninic acid assay

PBS phosphate buffered saline

PBST phosphate buffered saline – 0,1% tween

FBS fetal bovine serum

PEG polyethylenglycole

TBS Tris-buffered saline

TBST Tris –buffered saline – 0,1% tween

SGM second generation maleimide

DMF dimethylformamide

# 1. INTRODUCTION

## 1.1 Breast cancer

Breast cancer (BC) is the second most common cancer type, and a leading cause of death among women (Siegel et al., 2020). BC is a biologically complex and heterogeneous illness that arises in the lining epithelium cells of the ducts (85%) or lobules (15%) in the glandular tissue of the breast (**Figure 1**) (World Health Organization, 2021). The survival rates for BC exhibit variations according to the diagnosis stage, the molecular type of tumor, the grade of cancer (how fast it is growing), age, overall health, respond to treatment and so on. The general 5-year relative survival rate for breast cancer stands at 90%. The 5-year relative survival rates for each cancer stage are: 1) localized breast cancer (only in the breast tissue) is 99%, 2) regional breast cancer (has spread to nearby tissue or lymph nodes) is 86%; and 3) distant breast cancer (has spread to other parts of the body) is 28% (World Health Organization, 2021; WebMD, n.d., 2022). Different BC molecular subtypes have been identified thanks to gene array technology (Pupa et al., 2021). Based on the presence or absence of molecular markers for the estrogen or progesterone receptors and human epidermal growth factor 2 (HER2; also known as ERBB2), breast cancer is categorized into three major subtypes: hormone receptor positive/HER2 negative (70% of patients), HER2 positive (15%-20%), and triple negative (tumors lacking all three standard molecular markers; 15%) (Waks et Winer, 2018). A better comprehension of their biological heterogeneity could result in the creation of more potent therapeutic approaches (Pupa et al., 2021). As a result, preclinical investigations have shown that effective anticancer therapies must concentrate on aiming at numerous unique and nonredundant cell pathways in the various molecular BC subgroups.

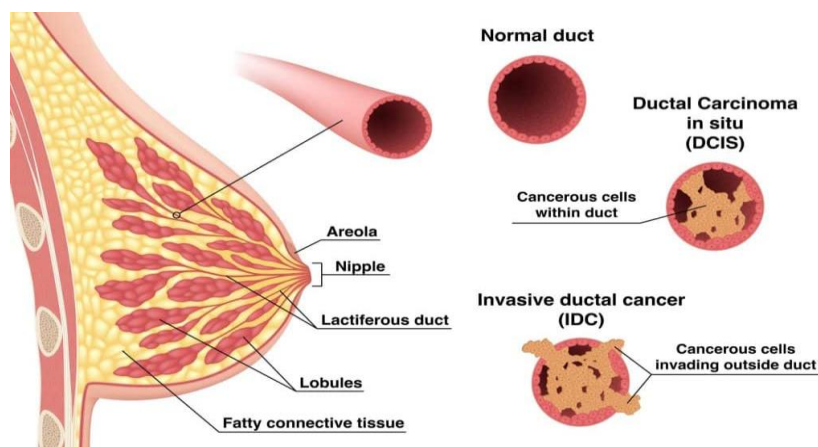


**Figure 1.** Schematics of *in situ* and invasive ductal carcinoma (TeachMeSurgery. (n.d.). Breast Carcinoma *In Situ*. TeachMeSurgery. Retrieved from <https://teachmesurgery.com/breast/malignant-disease/breast-carcinoma>)

At the time of diagnosis, more than 90% of breast cancers patients do not have metastatic disease (Hamer et Warner, 2017). Therapeutic objectives for patients without metastatic disease include the elimination of the tumor and minimizing recurrences. Most patients will undergo surgery to remove the tumor and/or the entire breast and have sentinel lymph node checked for infiltration of tumors cells. Systemic therapy for non-metastatic breast cancer is determined by subtype. Patients with hormone receptor-positive tumors receive endocrine therapy, with a small percentage also receiving chemotherapy; those with HER2-positive tumors get HER2-targeted antibody or small-molecule inhibitor therapy in addition to chemotherapy; and the ones with triple-negative tumors get chemotherapy alone. All patients with nonmetastatic breast cancer will get surgical resection as their local therapy, with postoperative radiotherapy being taken into account if a lumpectomy is performed (Waks et Winer, 2018).

### **1.1.1. HER2-positive breast cancer**

About 15% to 20% of BC cases include *HER2* overexpression or amplification, which represents a very aggressive subtype of BC (Loibl et Gianni, 2017). HER receptors include four structurally related members that occupy the cell surface; HER1 (ERBB1, also referred to as EGFR), HER2 (ERBB2), HER3 (ERBB3), and HER4 (ERBB4) (Dhritlahre et Saneja, 2021). All these receptors form dimers (forming ten different homo- and heterodimers; **Figure 2**). However, HER2-mediated heterodimerization is a reliable and potent signal transduction route (Murphy et Morris, 2012). The dimerization activates complex biological signaling pathways like the phosphatidylinositol 3-kinase/protein kinase B (PI3K/Akt) and mitogen-activated protein kinase / extracellular-related kinase  $\frac{1}{2}$  (MAPK / ERK1/2) pathways (Dhritlahre et Saneja, 2021). HER receptors comprise three domains: an extracellular ligand-binding domain (ECD), a lipophilic transmembrane domain, and, except for HER3, an intracellular tyrosine kinase domain (Dhritlahre et Saneja, 2021). The tyrosine kinase domains are activated by both, homodimerization and heterodimerization, usually induced by the binding of ligand (Hudis, 2007). Cell proliferation, survival, migration, angiogenesis, and metastasis are all resulting effects of these signaling cascades. Human Epidermal Growth Factor Receptor 2 (HER2), also known as ERBB2, is a 185 kDa protein with a crucial role in healthy cells during every stage of

cell development. *HER2* mutation and/or overexpression can initiate tumorigenesis and metastasis (Dhritlahre et Saneja, 2021). The *HER2* gene is overexpressed and amplified in human malignancies such as breast, gastric, ovarian, prostate and lung (Budi et al., 2022) making it an attractive target for cancer therapy.

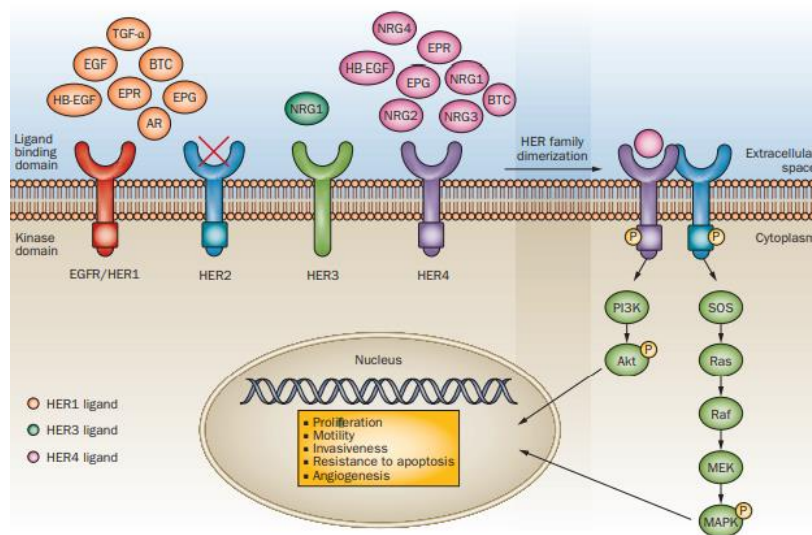


**Figure 2.** *HER family member heterodimer formation and downstream signaling. Signaling downstream of HER family activation depends on the heterodimerization of the HER family member initiated by ligand binding to the extracellular ligand-binding domain. An exception there is HER2 which has no known ligand and is always in an open conformation that permits dimerization (Arteaga et al., 2012)*

Patients with HER2-positive breast cancer have a considerably lower overall survival rate and a shorter relapse time than patients without HER2 overexpression. Studies conducted *in vitro* revealed that the suppression of the HER2 expression significantly induced breast cancer cells apoptosis (Engel et Kaklamani, 2007). Additionally, it has been proven *in vitro* that HER2-positive breast cancer cells experienced growth inhibition and apoptosis when their expression was reduced by antisense or siRNA (Faltus et al., 2004). Altogether, these findings point to the essential role of HER2 in proliferation and anti-apoptosis in HER2-positive breast cancer, suggesting that HER2 is an interesting therapeutic target for breast cancer treatment.

The essential tool in clinical practice for the detection of HER2-positive BC is the immunohistochemistry (IHC) due to its high specificity, sensitivity, reproducibility and cost-effectiveness (Moelans et al., 2011). However, it does have certain limitations, which include

subjectivity of interpretation, variability in staining quality, lack of standardized scoring system, heterogeneity within tumors, false-positive or false-negative results (Furrer et al., 2015). Despite these limitations, IHC is considered as a gold standard in the detection of HER2-positive breast cancers, and efforts are continually made to address these challenges.

### 1.1.2. Targeted therapy for the treatment of HER2+ breast cancer: focus on Trastuzumab

The first Food and Drug Administration (FDA)-approved targeted therapy for breast cancer was based on the use of Trastuzumab (Trz; also known as Herceptin). This recombinant humanized monoclonal antibody directed against HER2, developed by Genentech Inc (San Francisco, CA, USA) (Vu et Claret, 2012) constitutes one of the major achievements in clinical oncology and a strong proof of the efficacy of molecularly targeted therapies in BC (Liobl et Gianni, 2017). Trastuzumab is constituted by two antigen-specific sites that are attached to the juxtamembrane part of the extracellular domain of the HER2 receptor (Hudis, 2007). Trastuzumab inhibits the HER2 signaling by a number of different mechanisms, such as the blocking of the PI3K-AKT signaling pathway by obstructing the activation of its intracellular tyrosine kinase, by preventing the dimerization of the HER2 receptor, by the receptor internalization and/or degradation, by the recruitment of the immune effector cells through Fc receptors leading to an antibody-dependent cell-mediated cytotoxicity (ADCC) (**Figure 3**) (Dhritlahle et Saneja 2021). Additionally, Trastuzumab, when bound to HER2, prevents the extracellular domain of HER2 receptor to be cleaved by proteases, which lowers the levels of the more active p95-HER2 version of HER2 (Gajria et Chandarlapaty, 2011).

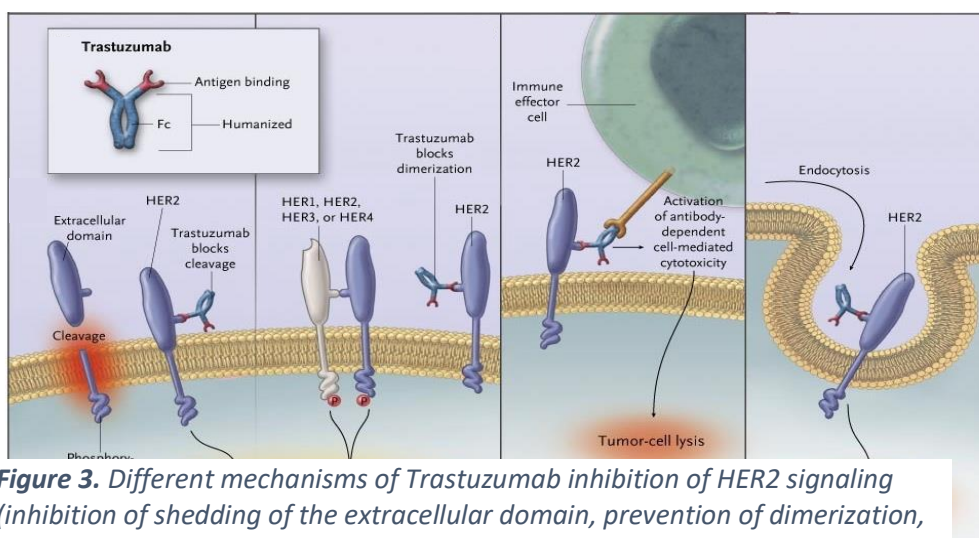


**Figure 3.** Different mechanisms of Trastuzumab inhibition of HER2 signaling (inhibition of shedding of the extracellular domain, prevention of dimerization, activation of ADCC, degradation of HER2 receptor). (Hudis, 2007)

## **1.2. Near infrared imaging**

### **1.2.1. Fluorescence properties and advantages in biological conditions**

NIR light is a type of electromagnetic radiation with wavelengths in the range of 700-1700 nm. Nowadays, an increasing attention has been drawn on NIR imaging in the biomedical field due to several advantages over traditional imaging in the visible region.

First, the use of NIR fluorescence allows a signal detection in an environment with an absence or low disturbance due to native fluorescence arising from cells and tissues, which mainly occurs in the visible region, which is named autofluorescence, and constitutes a significant source of background noise for bioimaging (Figure 4A.). Indeed, biomolecules constituting biological tissues, show very low absorption coefficients in the NIR spectrum windows (650-900 nm wavelengths) (Xu et Shang, 2018; Figure 4B.). In addition, an excitation with longer wavelengths has the advantage of reducing light scattering that results from the interaction with the diverse component of biological tissues. As a result, NIR light can penetrate through tissue up to a significant depth, estimated to multiple centimeters across heterogeneous living tissues, and that allows the collection of images with an enhanced resolution (Shang et al, 2011; Figure 4C)). Therefore, using detection in the NIR increases the signal-to-noise ratio, making it possible to obtain complex information with high temporal and spatial resolution through a non-destructive and multidimensional approach (Peng et al., 2020).

Finally, this technique does not involve ionizing radiations, is quite inexpensive and requires only small quantities of imaging agents.

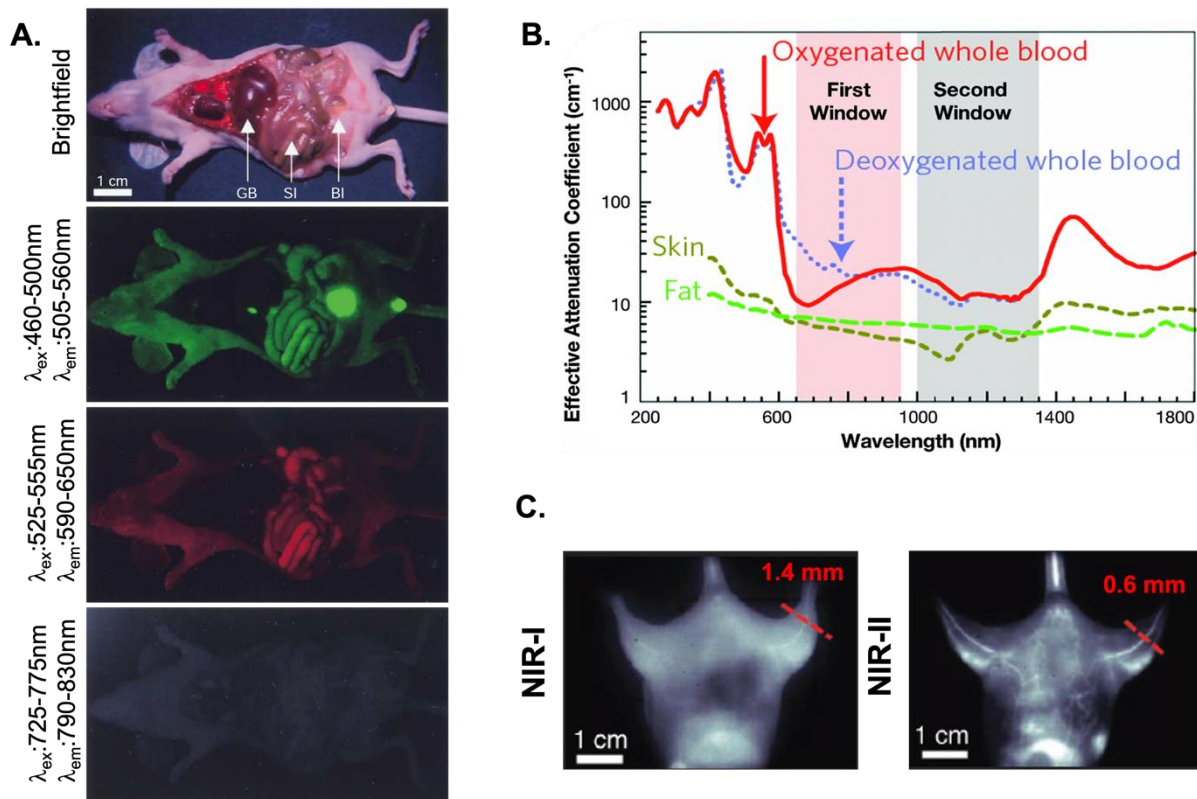


**Figure 4** : **A.** Wavelength-dependent autofluorescence of different tissues and body fluids in athymic *nu/nu* mice. Arrows mark the location of the gall bladder (GB), small intestine (SI) and bladder (BI). (Adapted from J.V. Frangioni, *Curr. Opin. Chem. Biol.* 2003) **B.** Plots shows effective attenuation coefficient (on a log scale) versus wavelength demonstrating lower absorption and scattering from oxygenated blood, deoxygenated blood, skin and fatty tissue in either the first (pink shaded area) or second (grey) near-infrared window (Adapted from AM Smith et al, *Nature Nanotechnol.* 2009) **C.** NIR-I and NIR-II fluorescence imaging of blood vessels in the mouse (Adapted from G. Hong et al., *Nat Med.* 2012)

Thus, fluorescence optical imaging in the near infrared (NIR) region is a powerful and highly sensitive tool with various *in vivo* and *in vitro* applications for preclinic and clinic studies.

### 1.2.2. Development of fluorescence guided surgery

Surgery is crucial for the treatment of solid cancers. Real-time intraoperative guidance is an emerging technique that is essential during oncological surgery to outright and safely remove tumors and, to preserve as much healthy tissue as possible. In oncology, clear margins after surgery is considered as the best prognosis factor. X-ray, positron emission tomography (PET), single photon computed tomography (SPECT), or MRI imaging techniques do not provide intraoperative guidance in real time and they are mostly used in operational planning (Hernot et al., 2019). The characteristics of NIR optical imaging make it an excellent method for conducting fluorescence imaging in real-time during surgical procedures. When the imaging resolution is sufficiently optimized, it has a great potential to enhance the visualization of

tumors during surgery, leading to a more precise tumor removal while minimizing harm to surrounding healthy tissues (Keereweer et al., 2011).

Fluorescence imaging applies a certain fluorescent agent for the sensitive visualization of the organ or tissue of interest. A fluorescent contrast agent is excited with an appropriate light source and the emitted light is captured by charge coupled (CCD) camera. Fluorescent imaging agents that emit at wavelengths comprised between 650-800 nm, in the near-infrared region, are preferable for medical applications, compared to those emitting visible light, to limit the contribution of tissue autofluorescence ameliorating the signal to noise ratio and the resulting image quality as stated in the previous paragraph (Hernot et al., 2019). In addition, an important effort has been made to miniaturize instruments to easily transport them to the patient bedside. Nowadays, compact open-field device or laparoscopic or robotic instruments can be integrated in all imaging equipment for contact-free interrogation in real time. In addition, the material cost has drastically decreased, making it accessible to a large number of hospital (Figure 5).

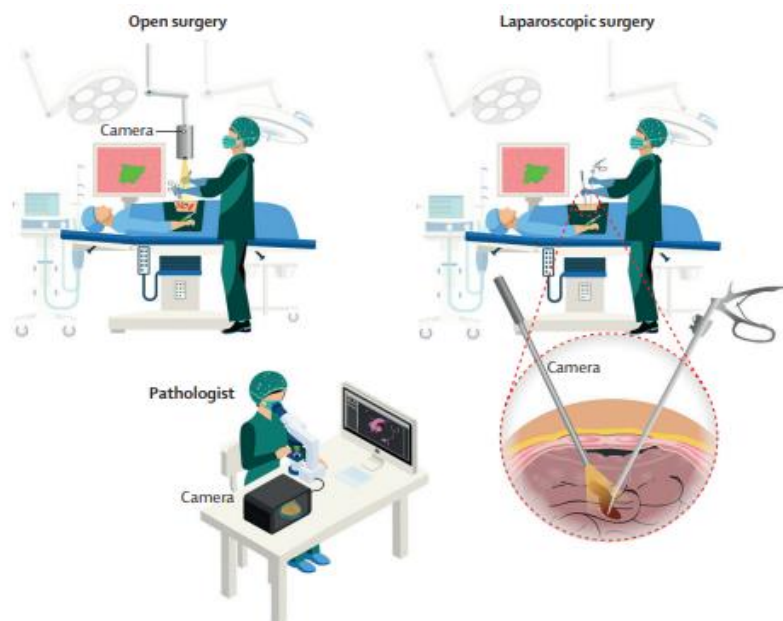


**Figure 5 :** Principle of intraoperative molecular NIR fluorescence imaging. Fluorescence guidance implemented in open or laparoscopic surgery. The tumor or other tissues can be visualized with a NIR camera after intravenous injection of the tracer 1 h up to several days before surgery, depending on the nature of the tracer. The surgeon is thereby guided in real-time during the resection. Directly after resection, pathologist can analyze tissue sample with a fluorescence camera and microscope to give brisk feedback to the surgeon about resection margins on the presence of fluorescence (adapted from Hernot et al., 2019).

The currently most commonly used approach is the passive targeting strategy utilizing the enhanced permeability and retention (EPR) effect. The indocyanine green (ICG) has been approved decades ago and has shown to be partially successful in clinical application for mapping lymph nodes, detecting gliomas, liver cancer and breast cancer. Another example is the 5-aminolevulinic acid (5-ALA), a heme precursor metabolized in fluorescent porphyrin by epithelial and cancer cells, which has demonstrated efficacy in performing and resecting intracranial tumors, bladder tumors and gastric cancers (Hi et Jiang, 2016). However, they encounter limitations such as:

- (i) The passive accumulation in tumors increasing the risk of false positive
- (ii) The low penetration depth of a few millimeters due to the significant absorption of light by biological tissues
- (iii) The important photobleaching and short excited lifetime increasing the risk of false negative that has been partially countered by the constant infusion of the product during surgery (with a risk of patient hypersensitivity)
- (iv) The presence of high levels of background light and autofluorescence contributing to a low signal-to-noise ratio (Xi et Jiang, 2016)

Efforts have been made to develop tumor-targeting contrast agents to increase specificity (Wu et al., 2021). However, these new molecules do not address the main problems of low penetration, photobleaching and contrast.

### **1.2.3. Luminescent lanthanide: Advantages and Challenges**

In recent decades, there has been significant focus on probes that contain lanthanide (III) ions ( $\text{Ln}^{3+}$ ). Particularly, the probes containing lanthanide that emit near-infrared light such as  $\text{Yb}^{3+}$ ,  $\text{Nd}^{3+}$ ,  $\text{Sm}^{3+}$ ,  $\text{Pr}^{3+}$ ,  $\text{Tm}^{3+}$ ,  $\text{Er}^{3+}$ , have found applications for biological imaging (Martinić et al., 2017).

The lanthanide series encompasses 15 elements ranging from lanthanum (La) to lutetium (Lu), with atomic numbers 57 and 71. These elements are classified under the f-block of the periodical table and the most common (the most stable) oxidation state for all lanthanide cations is +3.

Lanthanide ions have been widely used as luminescent probes due to their unique optical properties, including extended luminescent lifetimes, sharp emission bands with emission wavelengths that are not affected by the experimental conditions (temperature, pressure, pH, biological environment), large energy difference between excitation and emission wavelengths (Wang et al., 2014; Eliseeva et al., 2022). The long-lived luminescence of lanthanide ions can be captured through time-resolved fluorescence measurement, effectively removing the background interference (Wang et al., 2014). Consequently, these probes have found extensive domains of applications in areas such as bioanalytical detection, diagnosis and bioimaging.

The luminescence of free lanthanide ions is generally weak due to their low absorption coefficients. However, the lanthanide ions can be indirectly excited through a process called “sensitized emission” or “antenna effect”. This effect involves transferring the energy obtained from the absorption of the excitation light with an energy-harvesting antenna component to the lanthanide ions, populating their excited state (Aulsebrook et al., 2018). Lanthanide compounds can be considered as molecular devices that convert light, initially absorbed by the chromophoric ligand, into emitted light by the lanthanide ions through an intramolecular energy transfer process (Sabbatini et al., 1996).

To avoid the deactivation of lanthanides cation by water in biological environment, strategies have been developed to protect lanthanide ions in small molecules, macromolecules, metal-organic frameworks (MOF) or nanomaterials. Metallacrowns (MCs) are coordination-based self-assembled polynuclear complexes that have attracted considerable attention since 1989, when Pecoraro and Lah reported the first MC structure (Mezei et al., 2007; Ostrowska et al., 2016). MCs are structural analogues to organic crown ethers (**Figure 6**), that differ by the inclusion of a metal-heteroatom coordination units,  $- [M - N - O] -_n$  (repeating motif) replacing methylene groups. This coordination unit contains oxygen atoms that are capable of binding cations within their central cavity (Ostrowska et al., 2016).

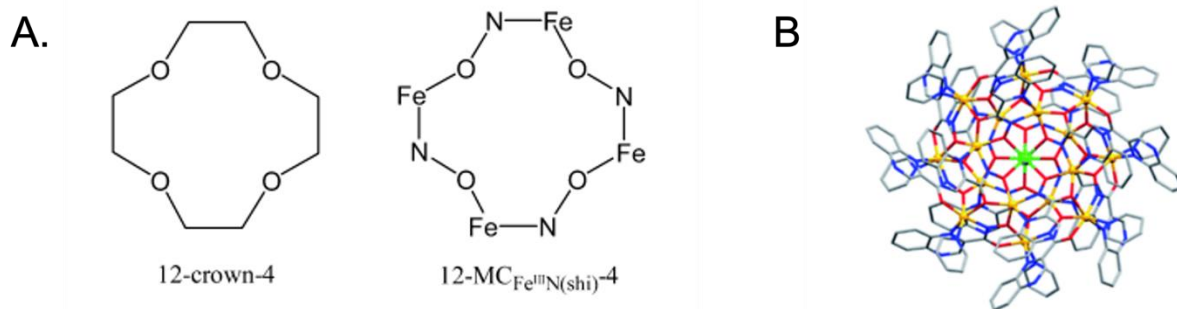


**Figure 6 :** **A.** Pictures showing the analogy between organic crown ethers and metallocrowns (Mezei et al., 2007). **B.** Molecular structure of the Zn<sub>16</sub>Yb(quinoHA)<sub>16</sub> MC obtained by single crystal X-ray diffraction. Color code: green, Yb; yellow, Zn; red, O; blue, N; grey, C. H atoms and solvents have been omitted for clarity (Eliseeva et al., 2022).

Ln<sup>3+</sup> Metallocrowns (MCs) are a unique class of Ln<sup>3+</sup> macrocyclic compounds which can encapsulate Ln<sup>3+</sup> into their -[M-N-O]<sub>n</sub>- cycle, where M is a transition metal ion from the d block elements. Ln<sup>3+</sup> MCs have demonstrated an exceptional ability to efficiently sensitize the characteristic emissions of Ln<sup>3+</sup> in the visible and NIR range (Eliseeva et al., 2022). Our group has established a strategy to encapsulate Ln<sup>3+</sup> MCs in NH<sub>2</sub>-functionalised polystyrene beads through a rapid swelling process, allowing the internalization of a large number of NIR emitting lanthanide and sensitizers per unit of volume. This approach allows the emission of a very large number of NIR photons, thus counteracting the detrimental effect of limited quantum yields of lanthanide ions. The newly developed approach shows great promise and can be extended to rapidly screen for sensitizers suitable the sensitization of the various NIR-emitting Ln<sup>3+</sup> ions. Additionally, such strategy can be used to create specific and sensitive imaging agents that emit NIR light.

### 1.3. Objective

The global objective of this project is the creation of innovative fluorescence-based imaging agent emitting in the NIR domain, which are versatile, easy to use, specific to a targeted tissue, and that allow the limitation of the risks of false positives or false negative. The NIR luminescent lanthanide –based probes possess the required desirable qualities to achieve this goal, such as emissions as sharp bands that do not overlap, with NIR wavelengths that allow sensitive detection. Within this project, my internship included three steps. i) The first step was the identification and selection of the most suitable cell line models for *in vitro* assays. ii) The preparation of the anti-HER2 probe was guided through the chemical conjugation of Trz to polystyrene beads. Before finalizing the complete conjugation, the following steps were

performed: coupling of the linkers to the beads (first with empty beads and then with beads containing Ln-based metallocrowns) followed by the reduction of the antibodies. iii) The third step was to test anti-HER2 conjugated beads *in vitro* in the studies of affinity, cytotoxicity, proliferation and NIR microscopy imaging on living cells.

## 2. MATERIALS AND METHODS

### 2.1. Cell lines

The HER2-positive (HER2<sup>+</sup>) breast cancer cell lines BT474 (ductal carcinoma) and triple negative MDA-MB-231 (adenocarcinoma) were ordered from American Type Culture Collection (ATCC, Manassas, VA, USA). Cells were cultured at 37°C, 5% CO<sub>2</sub> in growth medium Dulbecco's modified Eagle medium (DMEM) medium supplemented with 10% Fetal Bovine Serum (FBS), 50 U/mL penicillin, and 50 µg/mL streptomycin (Gibco, Life Technologies, CA, USA). The cells were pre-cultured prior to experiments until an 80% confluence was reached. The cells were harvested using Trypsin-EDTA 0,05% (Gibco, Life Technologies, CA, USA). After complete detachment, the cells were rinsed and resuspended in growth medium. The cell concentration was determined using a Neubauer counting chamber.

### 2.2. Bioconjugation of Trastuzumab and polystyrene beads

Humanized monoclonal antibody Trastuzumab (Trz) was obtained from the local hospital (@21mg/mL, Hôpital de la Source, Orléans, France) and was desalted in PBS using high performance gel chromatography resin columns (Zeba™ Spin Desalting Columns, 5mL, Thermo Fischer Scientific, USA). Trz was reduced with 5 or 10 equivalents of bond-breaker TCEP solution (MW: 250,2 g/mole, 0,5 M, Thermo Fischer Scientific, MA, USA) and the reaction mixture was stirred at 37°C for 2 hours. The reduction of the antibodies was checked on non-denaturing 12% acrylamide gel using 12µg of Native and TCEP reduced Trz. NH<sub>2</sub>-coated polystyrene beads (Size: 100 nm, Micromer, Germany), empty or containing Zn(II)/Yb(III) metallocrowns were linked via an NHS coupling to (MeO-(PEG)<sub>3</sub>-NHS (20 mM, MW=333,33 g/mole) and Mal-(PEG)<sub>6</sub>-NHS (20 mM, MW=601,6 g/mole). Briefly, 10 mg/mL of NH<sub>2</sub>-coated beads were washed in 10 mM PBS (pH7.4) and 600 µg of linkers was added (1:1 or 8:2 condition MeO-(PEG)<sub>3</sub>-NHS: Mal-(PEG)<sub>6</sub>-NHS ratio) for a 1-hour reaction at room temperature under mixing. After coupling, the excess of linkers was washed away twice with PBS followed by centrifugation (15000rpm, 30min) and resuspended in a sonication bath (15min, Fisherbrand, NH, USA). 10 mg of beads with linkers were immediately mixed with 1 or 2 mg of Trz and incubated during 2 hours at room temperature under mixing (**Figure 7**). The conjugated sample was centrifuged (15000 rpm, 30 minutes) to collect beads and flow-

through was used to measure the concentration of the remaining non-conjugated antibody using BCA assay (Pierce, Thermo Fisher Scientific, MA, USA).

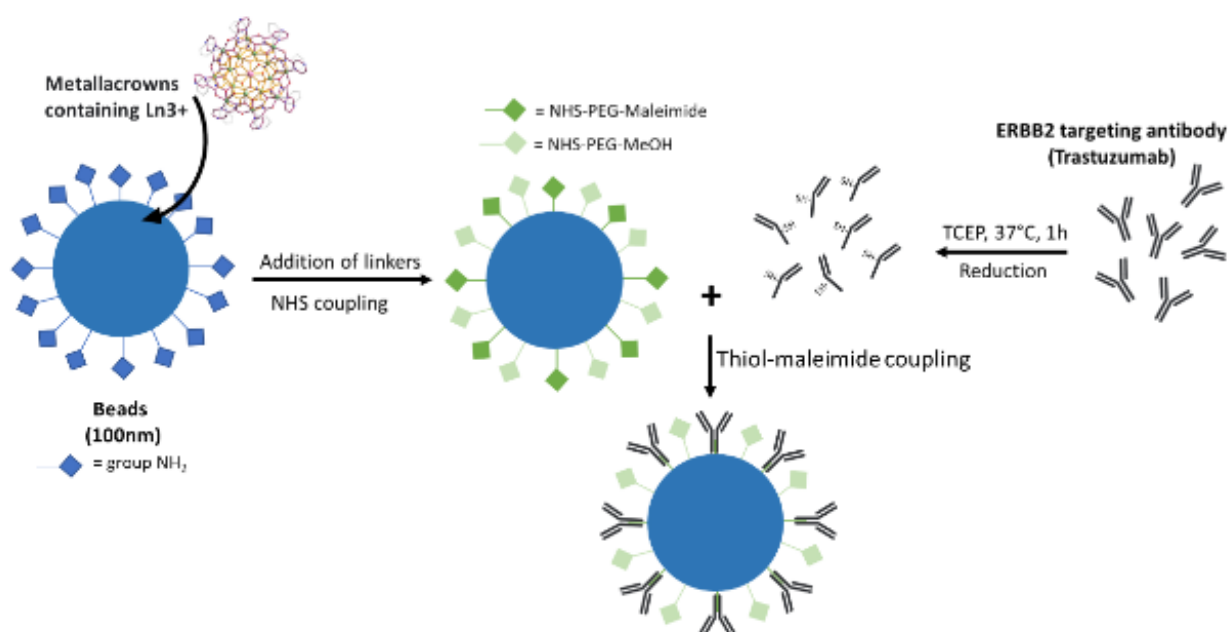


**Figure 7.** Schematic representation of the synthetic strategy used to create PEGylated PS beads and to conjugate with reduce HER2-targeting antibodies Trastuzumab.

### 2.3. Synthesis of the Zn<sub>16</sub>Yb(quinoha)<sub>16</sub> metallacrown and incorporation in polystyrene beads

The NIR emitting Zn<sub>16</sub>Yb(quinoha)<sub>16</sub> was prepared by Dr. Tu N. Nguyen using a self-assembly reaction between H<sub>2</sub>quinoha, Zn<sup>II</sup>, and Yb<sup>III</sup> in a DMF/H<sub>2</sub>O/pyridine solution that we have described previously (Eliseeva, 2022). The metallacrown has been incorporated in the polystyrene beads by Ms. Codruta C. Badescu-Singureanu.

### 2.4. Concentration of coupled antibodies

The quantification of the remaining non-conjugated antibodies (proteins) coupled to polystyrene beads was performed in triplicate using the Pierce™ BCA Protein Assay Kit (Thermo Fischer Scientific, MA, USA) following the manufacturer's instructions. The Pierce™ BCA Protein Assay Kit uses well-known reaction of protein-inducing the reduction of Cu<sup>2+</sup> into Cu<sup>+</sup> in an alkaline environment referred to as the Biuret reaction. This assay also incorporates the use of bicinchoninic acid (BCA) to achieve a sensitive and specific colorimetric identification of cuprous cation (Cu<sup>+</sup>) (Thermo Fisher Scientific, BCA assay). The method was not used for the direct measurement of antibodies-conjugated beads because of the

interference amide bond created between the beads and the linkers with the BCA assay kit. NH-group will be able to coordinate copper ion which is essential to the BCA reaction and will induce an increase of the absorbance which interferes with the measurement of the antibodies concentration.

## **2.5. Enzyme-linked immunosorbent assay (ELISA)**

The affinity of Trz and Trz-Beads for the HER2 receptor was checked by ELISA on living cells. Briefly, HER2-positive BT474 cell lines were coated in a 96-well plate (30,000 cells/well) and incubated overnight at 37°C in a saturated humidity atmosphere (5% CO<sub>2</sub>). The cells were then fixed with a solution of 4% PFA. The saturation was carried out in a solution with 3% bovine serum albumin in phosphate buffer saline (BSA-PBS) for 1 h at room temperature and washed with PBS-Tween 20 (0,05%) and PBS prior to incubation with Trz / Trz-Beads from 50-0.01 nM and matching beads concentration ranging from 220.5-0.11 µg of beads in triplicates. Wells were then washed with PBS-tween 20 and PBS and incubated with 100 µL of protein-L-peroxidase (1.25 µg/mL) for 2 h at 37°C. After washing, peroxidase detection was performed using 100 µL of TMB substrate. The enzymatic reaction was stopped with the addition of 100 µL 1M HCl, and the absorbance was measured at 450 nm using a microplate reader (ClarioStar, BMG Labtech, Germany). Further, normalization of cell number was performed using Janus Green stain. The plate was washed with PBS-tween 20 and PBS and incubated with 50 µL/well of Janus Green solution and incubated at room temperature for 5 minutes in the dark. Wells were then washed three times with PBS. To stop the staining, each well was incubated with 100µL of 1M HCl at room temperature for 10 minutes in the dark. Results were recorded by measuring absorbance at 595 nm on the same microplate reader as previously mentioned.

## **2.6. Cytotoxicity assay**

The cytotoxicity of conjugates on BT474 and MDA-MB231 cells was evaluated by the utilization of the Alamar blue test (Rampersad, 2012). 10,000 BT474 cells/well and 3,000 MDA-MB231 cells/well were plated onto a 96-well black plate and maintained at 37°C in a saturated humidity atmosphere (5% CO<sub>2</sub>) until the following day. Cells were treated in triplicates with different concentration of Trz and Trz-Beads (100 – 0,01 µg/mL). 48 hours after treatment, Alamar blue (Thermo Fischer Scientific, MA, USA) was added in each well and incubated 24 hours at 37°C in the cell culture incubator, protected from light. H<sub>2</sub>O<sub>2</sub> (200 nM) was used as a

positive control of toxicity. Results were recorded using a fluorescence excitation wavelength at 560 nm and an emission wavelength at 590 nm on a CLARIO Star microplate reader (BMG Labtech, Germany). The percentage of cell viability is calculated using the following equation:  
$$\% \text{ Viability} = ((\text{Mean OD}_{\text{treated sample}} - \text{Mean OD}_{\text{blank}}) / (\text{Mean OD}_{\text{negative (untreated) control}} - \text{Mean OD}_{\text{blank}})) \times 100).$$

## 2.7. Cell proliferation assay

BT474 and MDA-MB231 cells were seeded in triplicates at a density of 35,000 cells/well and 12,000 cell/well respectively and allowed to adhere and enter the growth phase before being treated with native Trz (10 µg/mL), Trz-Beads (10 µg/mL of bound Trz) or unfunctionalized beads in triplicates (same quantity of beads as in conjugated ones). After 7 days of treatment, cells were harvested by trypsinization and counted using the automated cell counter (NucleoCounter NC-250, ChemoMetec, Allerød, Denmark). The appropriate culture media, Trz, Trz-Beads and beads were replaced every 3 days.

## 2.8. Western blot

Cells were seeded in 6-well plates at a density of 300,000 cells for BT4747 and 100,000 cells for MDA-MB231 cell line and incubated overnight in the appropriate complete medium. Cells were treated with 10 µg/mL of native Trz or Trz-beads for 48 h. After PBS washes, cells were scraped in the presence of lysis buffer [50 mM Tris-HCl pH7.9, 40 mM NaCl, 1 mM MgCl<sub>2</sub>, 0.1% SDS and 1% Benzonase (Novus Biologicals, CO, USA)] supplemented with protease and phosphatase inhibitors (Thermo Fischer Scientific, MA, USA)] at 4°C.. Tubes were rotated on a wheel for 15 minutes at RT and vortexed. Protein extracts were quantified using the Pierce™ BCA Protein Assay Kit (Thermo Fischer Scientific, MA, USA), following the manufacturer's instructions. The samples were combined with 4x Laemmli loading buffer containing β-mercaptoethanol and boiled. Protein extracts were separated by SDS-PAGE (Biorad, CA, USA) and transferred on nitrocellulose membrane using a semi-dry transfer cell (OWL HEP-1, Thermo Fischer Scientific, MA, USA). Membranes were washed 3x with TBS-Tween 20 (0,1%) (TBS-T) and blocked with TBS-T containing 5% Bovine serum albumin (BSA) for 45 min at RT. After the blocking, membranes were incubated overnight with the primary antibodies diluted according to the manufacturer's instructions. After washing, membranes were incubated with a goat anti-rabbit IgG secondary antibody attached to peroxidase (HRP, Invitrogen, Thermo

Fischer Scientific, MA, USA) diluted in TBS-T containing 5% BSA for 1 h at RT. After several washes the proteins were visualized using an enhanced chemiluminescence system, Clarity™ Western ECL Substrate (Bio-Rad, CA USA), prior to the capture with the Western blot imager ChemiDoc MP Imaging System (Bio-Rad, CA, USA). Quantification was done using ImageJ software.

## **2.9 Luminescence spectroscopy**

These spectroscopic measurements were performed by Dr. Svetlana V. Eliseeva. Data were collected on freshly prepared suspensions of beads placed into 2.4 mm i.d. quartz capillaries. Steady-state emission and excitation spectra were measured on a Horiba-Jobin-Yvon Fluorolog 3 spectrofluorimeter equipped with a visible photomultiplier tube (PMT) (220-800 nm, R928P; Hamamatsu) and a NIR PMT (950-1650 nm, H10330-75; Hamamatsu). All spectra were corrected for the instrumental functions. Luminescence lifetimes were determined under excitation at 355 nm provided by a Nd:YAG laser (YG 980; Quantel), the signals in the NIR range were detected by the H10330-75 PMT connected to the iHR320 monochromator (Horiba Scientific). The output signals from the detectors were fed into a 500 MHz bandpass digital oscilloscope (TDS 754C; Tektronix) and transferred to a PC for data processing with the Origin 8® software. Luminescence lifetimes are averages of three or more independent measurements. Quantum yields were determined with a Fluorolog 3 spectrofluorimeter based on the absolute method using an integration sphere (GMP SA). Each sample was measured several times. Experimental error for the determination of quantum yields is estimated as ~10 %.

## **2.10. NIR epifluorescence microscopy**

Cells were seeded in 8-well Nunc Lab-Tek chambered cover glass (Thermo Fisher Scientific, MA, USA) at a density of 25,000 cells for BT4747 and 15,000 cells for MDA-MB231 cell line and incubated overnight in growth medium at 37°C in a 5% humidified CO<sub>2</sub> atmosphere. After 24h, the cell culture medium was removed and cells were washed twice with Opti-MEM (Gibco, Life Technologies, CA, USA) and incubated with 10nM, 25nM and 50nM of Trz coupled with PS beads containing Zn(II)/Yb(III) metallacrowns (**Figure 6B**) or the appropriate concentration of beads for 3 h. Prior to imaging, cells were washed twice with Opti-MEM to remove beads that were not bound specifically. Cells were observed using a Nikon Eclipse Ti fluorescence

inverted microscope equipped with a Photometrics EMCCD Evolve 512 camera (Roper Scientific, France) and acquired with the NIS-Elements software (Nikon). The light source, Nikon Intensilight C-HGFI, was combined with the filter cube combining the 377nm band pass 50nm filter for the excitation and 996nm band pass 70nm filter for the Yb<sup>3+</sup> emission in the NIR range (**Figure 8**).



**Figure 8.** Microscopy equipment that was used - Nikon Eclipse Ti fluorescence inverted microscope equipped with a Photometrics EMCCD Evolve 512 camera and acquired with NIS-Elements software

### 3. RESULTS

#### 3.1. Choice of cell lines

Five different cell lines were established and analyzed prior to the definitive implementation of the desired experimental methods. BT474 (ductal carcinoma) and ZR.75.1 (invasive ductal carcinoma) were established as HER2-overexpressing representative cell lines which also express estrogen receptor (ER<sup>+</sup>) and basic levels of progesterone receptor (PR<sup>+</sup>), BT20 (invasive ductal carcinoma) that is ER<sup>-</sup>, MCF-7 (invasive ductal carcinoma) with ER<sup>+</sup>, PR<sup>+/-</sup> and HER2<sup>-</sup> immunoprofile and MDA-MB-231 (adenocarcinoma) known as a triple-negative cell line (ER<sup>-</sup>, PR<sup>-</sup>, HER2<sup>-</sup>) (Burdall et al., 2003; Holliday et Speirs, 2011; American Type Culture Collection (n.d.)). Western blot results confirmed the previously published data suggesting that BT-474 is a good cellular model to study HER2 overexpression (**Figure 9**). In contrast, we decided to use MDA-MB-231 cells as negative control cell line as it is expressing a low level of MDA-MB-231, that could be close to endogenous level.

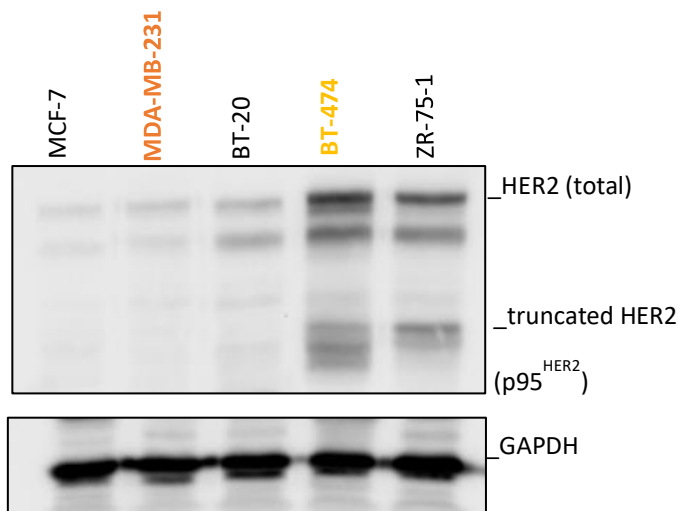


*Figure 9. Representative immunoblot staining for total HER2 and GAPDH (as loading control) in breast cancer cell lines MCF-7, MDA-MB-231, BT-20, BT-474, ZR-75-1.*

#### 3.2. Antibodies reduction and bioconjugation

The desalted humanized monoclonal antibody Trastuzumab (Trz) was reduced in a reaction using 5 or 10 equivalents of bond-breaker TCEP solution under stirring, either at room temperature or at 37°C, for 2 hours. The antibodies reduction was checked on non-denaturing

12% acrylamide gel using 12 $\mu$ g of native and TCEP reduced Trz. The gel was stained with Instant blue protein staining (Abcam, Cambridge, UK), (**Figure 10**). Results of reduction revealed different forms of reduced Trz: Trz without one light chain, Trz without two light chains, half of Trz (one light and one heavy chain) and heavy and light chains alone. The most appropriate forms of reduced Trz were obtained with 10 eq of bond-breaker TCEP solution at 37°C. These experimental conditions result in the lowest quantity of antibodies with nonfunctional antigen binding sites (Trz without light chains and heavy and lights chains alone) and the highest quantity of Trz with functional antigen-binding sites (Trz without just one light chain and halves of Trz antibodies).

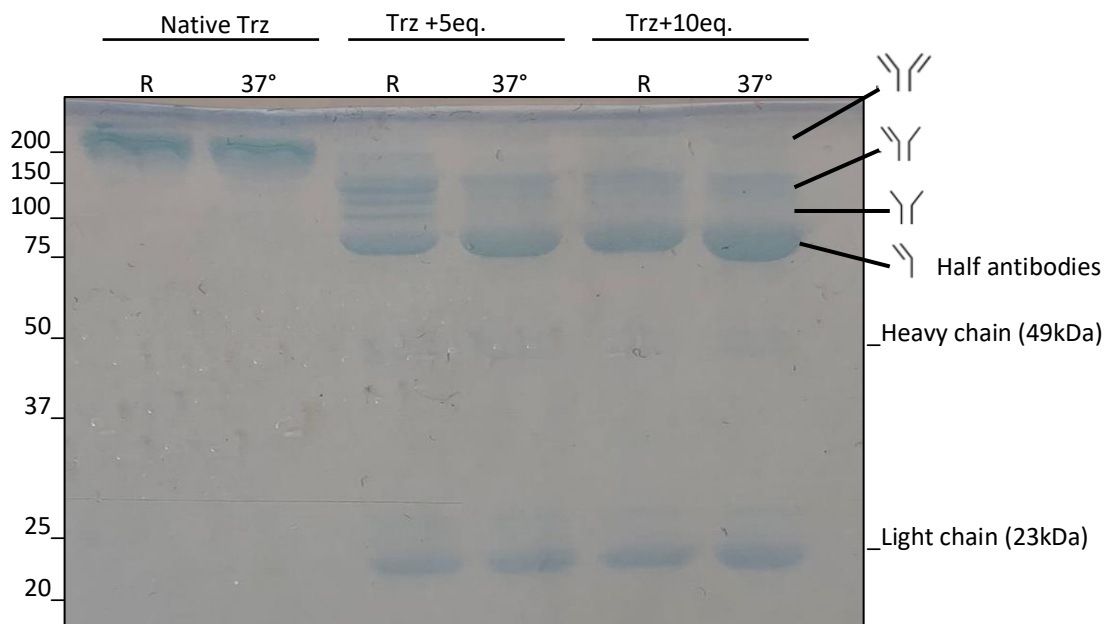


**Figure 10.** Representative gel staining for the reduction of Trastuzumab antibodies with different equivalents of TCEP solution and temperatures of reaction.

Further, the bioconjugation reaction of polystyrene beads with linkers and reduced Trz was performed under different conditions. 1:1 and 8:2 ratios of MeO-(PEG)<sub>3</sub>-NHS and Mal-(PEG)<sub>6</sub>-NHS linkers were used, as well as 1 and 2 mg of reduced Trz (**Table 1A**). Reactions were performed for 2 h and 24 h at room temperature, as well as for 2 h and 24 h at 37°C (**Table 1B**). Collected flow through fractions (FT) from centrifuged samples were analyzed in the BCA assay and the lowest concentration of non-bonded Trz was obtained in flow-through after 2 h reaction at the room temperature. Established conditions were considered as being optimal for further bioconjugation reactions.

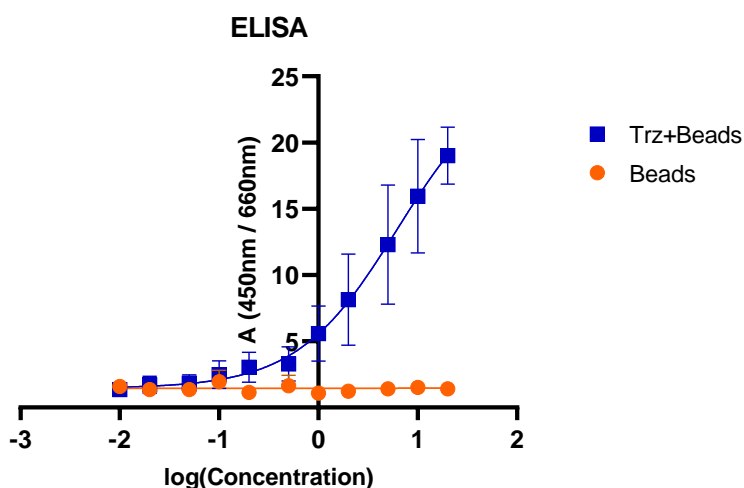
**Table 1.** Results of the bioconjugation efficiency under different conditions **A.** Table with different ratio of PEG linkers and antibodies; **B.** Table with different temperature and timing of reaction.

Table 1A			
Conditions		Results	
(PEG) <sub>3</sub> :(PEG) <sub>6</sub> linkers	Trz (mg)	Bonded Trz (µg/mL)	Bonded Trz (%)
1:1	1	135.70	13.57
<b>1:1</b>	<b>2</b>	<b>635.83</b>	<b>31.80</b>
8:2	1	49.32	4.93
8:2	2	430.99	21.55

Table 1B			
Conditions		Results	
Temperature	Time (hours)	Bonded Trz (µg/mL)	Bonded Trz (%)
Room temperature	<b>2</b>	<b>298.19</b>	<b>14.91</b>
37°C	2	66.83	3.34
Room temperature	Overnight	179.64	8.98
37°C	Overnight	98.85	4.94

### 3.3. ELISA

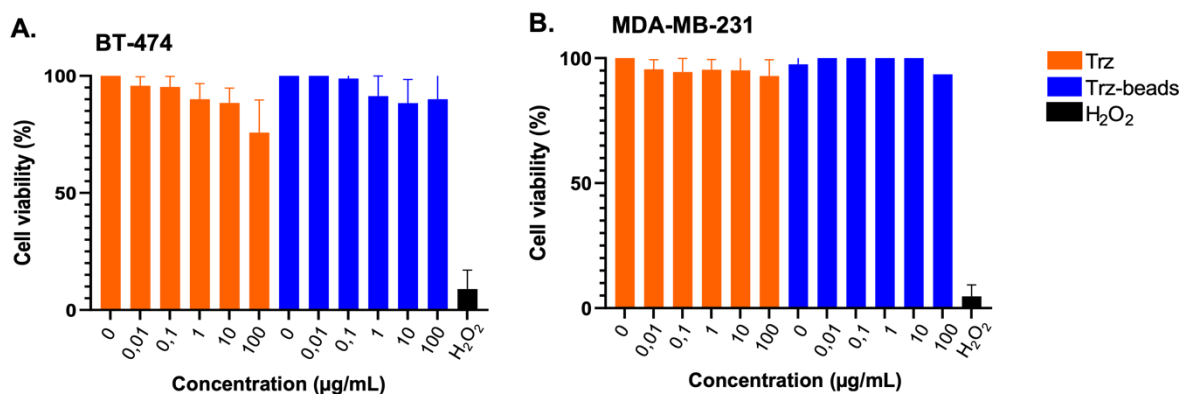
The efficiency of Trastuzumab coupled beads (Trz-beads) bound to HER2 was assessed by ELISA on cells. BT474, cell line that overexpress HER2 receptor, were seeded in 96 well plate and fixed before being treated with Trz-beads or unfunctionalized beads at different concentrations (20-0.01 nM). Cell number variations were normalized by using Janus Green cell stain solution. Antibodies binding affinity was preserved after coupling despite the antibodies reduction and coupling to much larger beads (radius = 100 nM). In contrast, no interaction of the unfunctionalized beads was detected (**Figure 11**).



**Figure 11.** ELISA test on BT-474 cells of the immunoreactivity of Trz-Beads (blue curve) vs. beads alone (orange curve). (n=3, with 3 technical replicates/experiment)

### 3.4. Cell viability

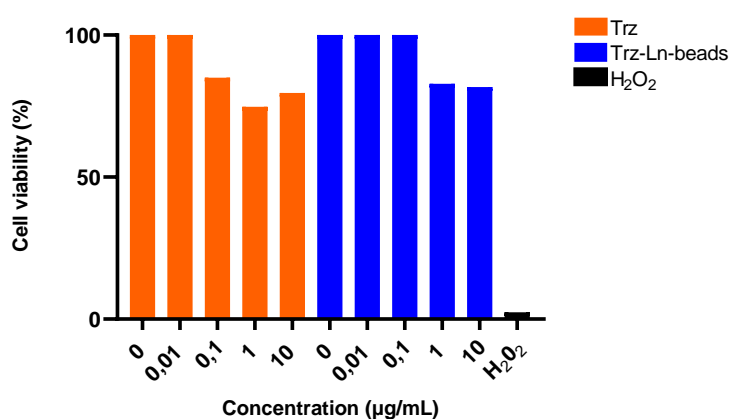
The cell viability was evaluated *in vitro* on HER2-overexpressing (BT474) and HER2-negative (MDA-MB231) cell lines to test the possible effects of the Trz and Trz- beads (Figure 12). Cells were treated with increasing amounts of Trz and Trz-beads (100-0.01  $\mu\text{g}/\text{mL}$ ). As a positive control, a dose of 10 $\mu\text{L}/\text{well}$  of 200 mM H<sub>2</sub>O<sub>2</sub> was used. 48 hours after treatment, Alamar blue was added and the fluorescence was measured 24 hours after.



**Figure 9.** Effects of Trz-beads and Trz (from 100  $\mu\text{g}/\text{mL}$  to 0.01  $\mu\text{g}/\text{mL}$  respectively) on the cellular viability, with H<sub>2</sub>O<sub>2</sub> treatment as positive control of A. BT474 and B. MDA-MB231 cell lines for 72 h. Data are expressed as mean  $\pm$  SEM. One sample t-test was used for statistical analysis. \*\*p  $\leq$  0.01 (n=3, with 3 technical replicates/experiment).

Overall, no significant cytotoxic effect was detected between the Trz-beads and the unfunctionalized beads upon treatments on BT4747 and MDA-MB231 cell lines. A similar experiment has been conducted with Trz-beads containing the matallacrown Zn<sub>16</sub>Yb(quinoHA)<sub>16</sub> (Trz-Ln-beads). No significant difference of toxicity has been shown in BT

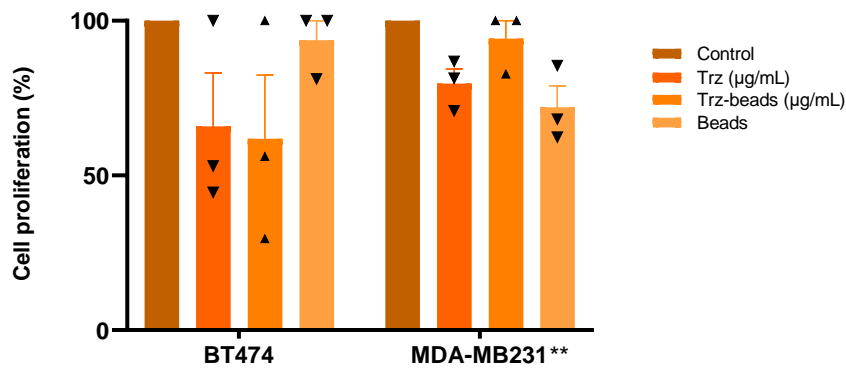
474 cells treated with Trz-Ln-Beads as compared to those treated with Trz. (Figure 13).



**Figure 10.** Effect of Trz and Trz-Ln-beads (from 10 µg/mL to 0.01 µg/mL respectively) on the cell viability, with H<sub>2</sub>O<sub>2</sub> treatment as positive control of BT474 cell line for 72 h. Trz-Ln-beads compound exhibit a concentration-dependent cytotoxic effect while a slight cytotoxicity was observed with higher concentrations of compound (1 and 10 µg/mL) resulting in a decrease in cell viability. Data are expressed as mean ± SEM (n=1, with technical triplicate).

### 3.5. Cell proliferation

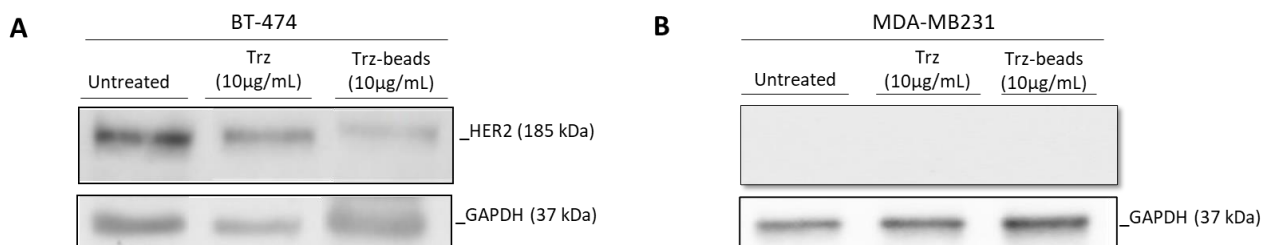
The antiproliferative potential of Trz, Trz-beads conjugates and unfunctionalized beads were determined *in vitro* on both, BT474 (HER2-overexpressing) and MDA-MB231 (HER2-negative) cell lines. Cells were treated with 10 µg/mL of Trz, Trz-beads and an equivalent quantity of unfunctionalized beads during 7 days. The number of living cells was determined with the automated cell counter and the percentage of proliferating cells is presented according to the control group (untreated cells) which has taken as completely proliferative (Figure 14). The treatment with Trz demonstrated an antiproliferative effect on both, the BT474 and MDA-MB231 cell lines. A moderate antiproliferative effect of Trz is indicated in the BT-474 cell line with approx. 65% of proliferating cells. The treatment with Trz-beads resulted in a further reduction in cell proliferation in the BT-474 cell line and non-significant reduction in MDA-MB231 cell line. These results suggest that the combination of Trz and beads could potentially enhance the antiproliferative effect, demonstrating a promising avenue for future investigations. Interestingly, treatment with beads alone resulted in a high percentage (~95%) of cells displaying active proliferation, indicating no significant antiproliferative effect. However, in the MDA-MB231 cell line, treatment with beads alone exhibited a moderate antiproliferative effect with ~75% of proliferating cells.



**Figure 11.** Effect of Trz, Trz-beads and beads on cell proliferation of BT474 and MDA-MB231 cell lines as percent of cell proliferation according to the number of living cells. Reorganized to have a graph for BT474 and for MDA-MB-231. Data are expressed as mean  $\pm$  SEM. One sample t-test was used for statistical analysis. \*\* $p \leq 0.01$  for MDA-MB231 cell line and n.s. for BT474; ( $n=3$ , with 3 technical replicates/experiment).

### 3.6. HER2 expression

Trz influence the level of total HER2 proteins due to its actions on signaling pathway involved in HER2 expression as well as its role in preventing dimerization and cell survival (Patel et Peng, 2020). Western blot was performed to investigate the level of expression of the HER2 receptor. A decrease in expression of HER2 receptor has been detected in BT474 treated cells with Trz (~9%) and Trz-beads conjugates (~5%) as compared to untreated cells; (\* $p < 0.05$ ; One-sample t-test; data expressed as mean  $\pm$  SEM) (**Figure 15**). Trastuzumab's action on HER2-negative cell line is non-existing due to lack of HER2 receptor overexpression. When Trz is bound to polystyrene beads, it exhibits a slightly lower anti-expressing effect on HER2 receptor compared to Trz alone. The binding of Trz to beads may modify the accessibility and availability of the antibody to interact with the HER2 receptor.



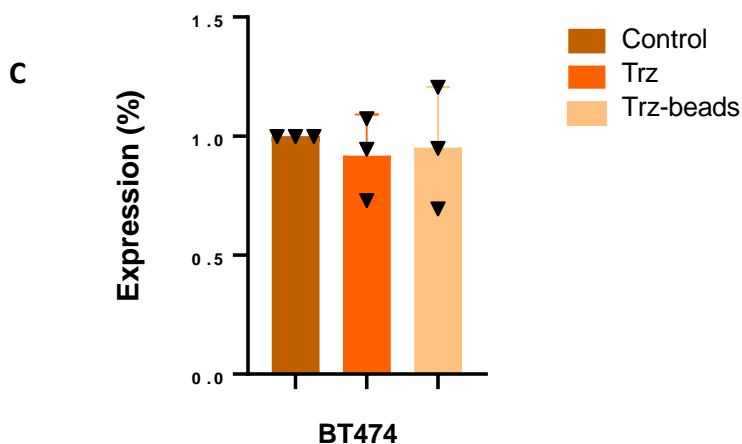
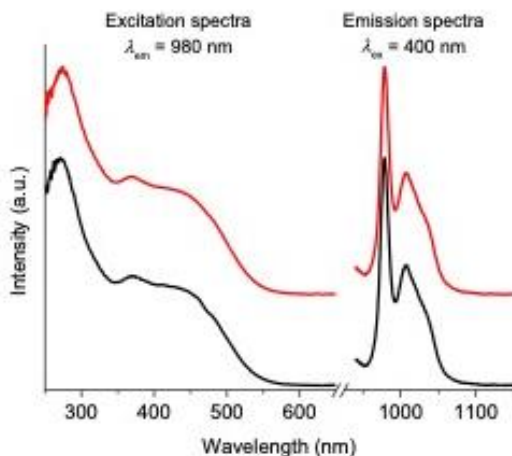


**Figure 12.** Representative results for decreased protein expression during treatment. Immunoblot of A. BT474 and B. MDA-MB231 treated with Trz, Trz-beads and without treatment for total HER2 and GAPDH. C. Quantification of HER2 expression on immunoblots of BT474 cell line treated with Trz, Trz-beads and without treatment (control). Data are expressed as mean  $\pm$  SEM. One sample t-test was used for statistical analysis. \* $p < 0.05$  ( $n=3$ , with 3 technical replicates/experiment).

### 3.7. Spectroscopic characterization of the conjugated beads containing the NIR emitting metallacrown.

The photophysical characteristics of PS NH<sub>2</sub>-coated beads were monitored after the incorporation of YbZn<sub>16</sub>(quinoHA)<sub>16</sub> and after Trastuzumab coupling by Svetlana Eliseeva using luminescence spectroscopy. As previously described for YbZn<sub>16</sub>(quinoHA)<sub>16</sub> (Eliseeva et al, 2022), excitation and emission spectra of YbZn<sub>16</sub>(quinoHA)<sub>16</sub>@PS/NH<sub>2</sub> and YbZn<sub>16</sub>(quinoHA)<sub>16</sub>@PS/Trz beads remains similar to YbZn<sub>16</sub>(quinoHA)<sub>16</sub> in the solid state. In addition, the quantitative photophysical properties such as luminescent lifetimes and absolute quantum yield are comparable to the ones previously obtained for YbZn<sub>16</sub>(quinoHA)<sub>16</sub> in methanol solution (respectively  $\tau_{obs}=22.6\mu s$  and  $Q_{Yb}=0,135$ ). YbZn<sub>16</sub>(quinoHA)<sub>16</sub> is insoluble in water. By incorporating YbZn<sub>16</sub>(quinoHA)<sub>16</sub> in beads, we were able to use this metallacrown as a suspension in water. Both luminescent lifetimes and absolute quantum yield remain constant after Trz conjugation. The incorporation of insoluble in water YbZn<sub>16</sub>(quinoHA)<sub>16</sub> into beads allow us to use it in biological system while maintaining their photophysical properties.

A.



B.

	$\tau_{\text{obs.}}$ ( $\mu\text{s}$ )	$Q_{\text{Yb}}$ (%)
$\text{YbZn}_{15}(\text{quinoHA})_{15}@\text{PS}/\text{NH}_2$	25.1(3)	0.116(1)
$\text{YbZn}_{15}(\text{quinoHA})_{15}@\text{PS}/\text{Trastuzumab}$	25.9(3)	0.137(1)

**Figure 16. A.** Corrected and normalized excitation and emission spectra of  $\text{YbZn}_{16}(\text{quinoHA})_{16}@\text{PS}/\text{NH}_2$  (black traces) and  $\text{YbZn}_{16}(\text{quinoHA})_{16}@\text{PS}/\text{Trz}$  (red traces), (1mg/mL suspension in water, room temperature). **B.**  $\text{Yb}^{\text{III}}$ -centered observed luminescence lifetimes and absolute quantum yields of  $\text{YbZn}_{16}(\text{quinoHA})_{16}@\text{PS}/\text{NH}_2$  and  $\text{YbZn}_{16}(\text{quinoHA})_{16}@\text{PS}/\text{Trz}$  (1mg/mL suspension in water, room temperature).

### 3.8. NIR epifluorescence microscopy

Beads containing  $\text{Zn}_{16}\text{Yb}(\text{quinoHA})_{16}$  MC were prepared by Codruta C. Badescu-Singureanu (PhD student in chemistry, working in the same team) (Figure 6), (Eliseeva et al., 2022). Conjugation of Trz to polystyrene beads containing Yb-metallacrown was performed according to previously described procedure. After successful binding, the luminescent conjugated complex was visualized under NIR epifluorescence microscopy. 24 hours after seeding cells in Nunc Lab-Tek chambered cover glass, BT474 and MDA-MB231 were treated with Trz-Ln-beads and Ln-beads for 3 h to verify the binding and the specificity (Figure 17). Cells were observed with fluorescence inverted microscope where the light source was selected with 377nm band pass 50nm filter for the excitation and a 996nm band pass 70nm emission filter to monitor specifically the  $\text{Yb}^+$  emission in the NIR range. The collected images confirmed the binding of Trz-Ln-beads to BT474, but also, to a lower extent as indicated by the faint NIR signal, MDA-MB231 even though this cell line is considered as triple-negative (ER-, PR-, HER2-), it does express basic levels of HER2 receptor.

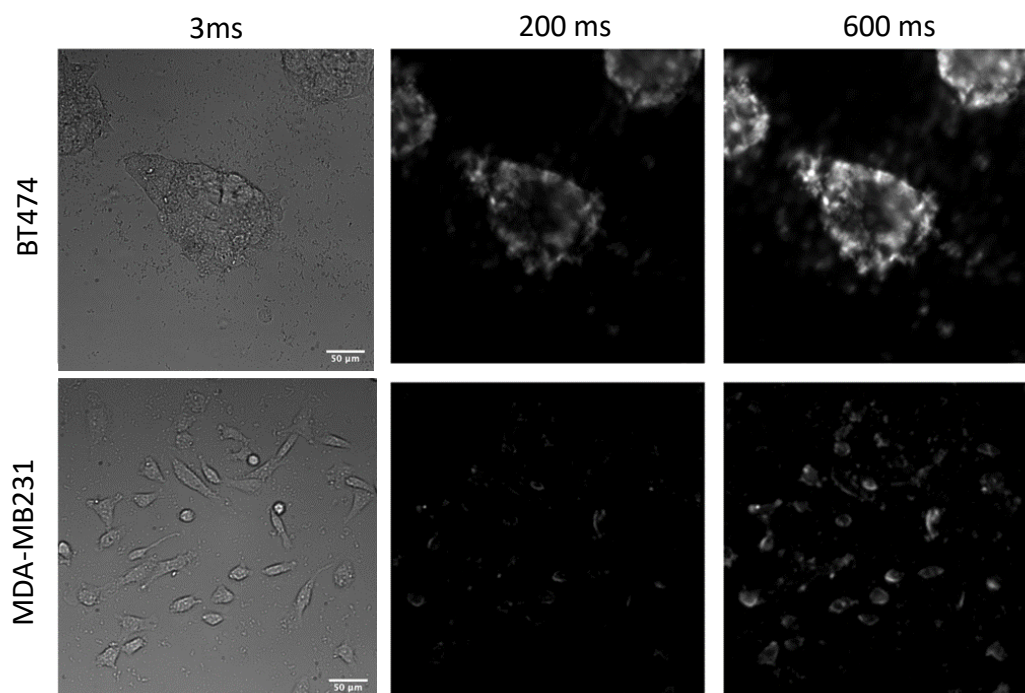


**Figure 17.** NIR epifluorescence microscopy images: the first column of pictures shows the bright field image (blank control to locate the living cells), second and third column show NIR luminescence images pictures using the following set of filters: BP377 (excitation), FF801 (dichroic) and BP996 (emission). The pictures shown in the second column were obtained with a 200 ms integration time and the pictures depicted in the third column pictures were obtained with a 600ms integration time. Magnification: x20.

#### 4. DISCUSSION AND CONCLUSIONS

Breast cancer remains one of the most spread malignancies worldwide and the HER2 positive breast cancer subtype constitutes 15 to 20% of this population. HER2 positive metastatic breast cancer remains an incurable condition despite the development and utilization of new recognition methods and therapies in our everyday clinical toolkit. Within this context, the primary aim of this project is to create and enhance an innovative imaging methods and reagents with higher specificity, sensitivity and accuracy that will allow an early detection and more efficient cancer removal.

We have developed new diagnostic tool based on polystyrene beads incorporating Ln-based metallocrowns emitting NIR light that were biologically targeted for the first time through a conjugation reaction with Trz. The bioconjugation reaction was performed under various experimental conditions: ratios of linkers, concentration of TCEP and reduced antibodies, temperature and coupling duration. Quantifications of the resulting bioconjugations revealed that the reaction corresponding to the lowest concentration of remaining / unreacted Trz correspond to a coupling that was reached after 2-hour reaction at room temperature, 1:1 linker ratio and 2mg of reduced trastuzumab with 10equivalents of TCEP. Furthermore, recent studies demonstrated that the utilization of the first generation maleimide (FGM) suffer from limited stability in serum (Nunes et al., 2015). To overcome this limitation, a second generation maleimide (SGM) has been developed, showing improved site-specificity of conjugation. Additionally, the numbers and positions of the conjugation sites on the antibody can influence the stability and the biological activity of the conjugate (Hervé-Aubert et al., 2018). The optimized protocol for the bioconjugation gave us approximatively 30% of coupled Trz to polystyrene beads (~600 µg/mL) which is more than enough for further experiments and optical microscopy imaging, which was later confirmed in this work.

The HER2 binding efficiency results obtained from ELISA assays confirmed that the binding of Trz-beads was preserved despite the potential coupling risks due to the antibodies reduction and the conjugation to large size particles (100 nm). Importantly, no significant interaction was observed with unfunctionalized beads, indicating the specificity of the Trz-beads conjugate for HER2-overexpressing cells. The viability of cells treated with different concentrations of Trz and Trz-beads was examined using the Alamar blue assay. An important

notice is that Trz should not cause apoptosis directly but should inhibit the proliferation of HER2-overexpressing cells by slowing down the progression of cell cycle and favoring the cell targeting by immune cells in the tumor microenvironment. Obtained results indicated that both Trz and Trz-beads treated BT474 cells and MDA-MB231 cells do not exhibit significant sign of cytotoxicity. The viability of cells treated with Trz-Ln-beads was also measured using the Alamar blue method and was expressed as a percentage relative to the control group. At concentrations of 0.01 and 0.1  $\mu\text{g/mL}$ , Trz-Ln-beads compound did not exhibit significant cytotoxic effects, with cell viability rates comparable to the control group. However, at concentrations of 1 and 10  $\mu\text{g/mL}$ , Trz-Ln-beads demonstrated a slight cytotoxicity, resulting in a decrease in cell viability. These findings suggest a concentration-dependent cytotoxic effect of Trz-Ln-beads on the BT474 cell line, with a significant cytotoxicity observed only at higher concentrations. Further investigation is warranted to elucidate the underlying mechanisms since these experiments could not be replicated due to lack of time for further analysis. Also, the cytotoxicity assay for beads and Ln-beads should be performed to show that there is no toxicity/release of metallacrown that would possibly harm cells. The potential antiproliferative effect of the tested compounds was determined by counting cells after a periodical treatment during 7 days with Trz, Trz-beads and unfunctionalized beads. The percentage of proliferating cells was presented relative to the control group. The results showed that Trz and Trz-beads significantly inhibited the proliferation of BT474 cells compared to the control group. In contrast, there was no significant effect on MDA-MB231 proliferation indicating again the high selectivity of Trz / Trz-beads for HER2-overexpressing cells. The results of Western blot confirmed the binding efficiency of Trz and Trz-beads and confirmed the inhibition of HER2 receptor expression. In addition, no binding was observed for the triple-negative cell line MDA-MB231, which does not overexpress the HER2 receptor. Additionally, the Western blot analysis revealed a decrease in the expression of the HER2 receptor in BT474 cells treated with Trz and Trz-beads conjugates, suggesting their potential as inhibitors of HER2 receptor signaling. This phenomenon can be explained by further mechanisms of action of Trz. As a matter of fact, Trz can trigger an immune response by the binding to HER2 which leads to the initiation of ADCC. This immune mediated cytotoxicity can lead to a reduction in the HER2 protein expression on the cell surface (Baselga et al., 1996). Trz binding to the HER2 receptor can also induce the internalization and the degradation of receptor complex followed by the lysosomal degradation, leading to the reduced HER2

signaling and downstream cellular proliferation (Sliwkowski et al., 1999). The HER2 receptor is also known to form heterodimers with the other members of EGFR family. The binding of Trz to the HER2 receptor can disrupt these heterodimeric interactions, thereby preventing the downstream signaling events (Molina et al., 2001). Collectively, these mechanisms contribute to the observed decrease in HER2 protein expression in the cell line that overexpresses the HER2 receptor when treated with Trz, which in our case is BT474.

Furthermore, after the successful binding of Trz to Ln-beads, the conjugated complex was tested *in vitro* and visualized using NIR epifluorescence microscopy. BT474 and MDA-MB231 cells were treated with Trz-Ln-beads and unfunctionalized Ln-beads to verify the binding and the specificity of the conjugates. NIR fluorescence inverted microscopy was used to observe the cells, with the light source combined with a filter cube that provides an excitation wavelength of 377 nm with a bandpass of 50 nm, and an emission wavelength of 996 nm with a bandpass of 70 nm to select the NIR signal of Yb<sup>+</sup>. The obtained images confirmed the binding of Trz-Ln-beads to BT474 cells, as a major proof of validity of our approach. The NIR images also revealed some level of unspecific binding of Trz-Ln-beads to MDA-MB231 cells. Beads showed some level of nonspecific binding despite of the double washing with Opti-MEM medium after treatment. These findings indicate that some optimization of the process is still needed such as stronger washing solution/medium that would be strong enough to wash out the entire amount of nonspecifically bound beads, but mild enough for the attached cells.

In summary, the results obtained in this work demonstrate the successful bioconjugation of Trz to polystyrene beads under optimized conditions. The Trz-beads conjugate exhibited a preserved binding affinity for HER2 and showed specific interactions with HER2-overexpressing cells. Furthermore, the Trz-beads conjugate did not display a significant cytotoxic effect but inhibited the proliferation of HER2-overexpressing cells without causing direct apoptosis. As a result, this work constitutes the first example of the use of a NIR-emitting metallocrowns for a targeted biological imaging in living cells through the connection to an antibody. It constitutes a major step forward for the group which has worked with such NIR-emitting metallocrowns for 10 years now. It opens promising perspectives for the application of these metallocrowns, the majority of which are not soluble in aqueous conditions.

These findings suggest the potential of Trz-beads as an innovative targeted diagnostic tool for HER2-positive breast cancer. However, it is important to acknowledge the remaining limitations of this study, including the low solubility of the (filled or empty) polystyrene beads. Also, the problem described above related to a limited remaining level of unspecific binding of Trz-Ln-beads should be addressed in the future. Further research and optimization of the conjugation process may help to overcome these limitations and enhance even more the high potential for applications of Trz-conjugates in targeted cancer diagnostic.

The hydrodynamic diameter of the tested beads, which is 100 nm, does not appear as a limitation here since similar types of beads are available with smaller and even bigger diameters which could allow different type of applications. These polystyrene beads also offer several advantages, such as their affordable cost, ease of manipulation, ability to control their properties, low or absence of cytotoxicity and the high potential for versatile functionalization. In comparison to other lanthanide (III) complexes and nanoparticles, these NIR-emitting beads provide attractive prospects for developing imaging agents that can be adapted to specific biological applications, including *in vivo* small animal imaging - that is in subcutaneous tumor in mice. Moreover, the proposed compound has possible future application in medical field, specifically for testing patient tumor biopsies in potential collaboration with the hospital. This collaborative effort aims to explore the potential of compound for advancing personal medicine with early detection and cancer removal.

## 5. REFERENCES

1. "Breast Cancer." World Health Organization. Retrieved from <https://www.who.int/news-room/fact-sheets/detail/breast-cancer>.
2. American Type Culture Collection (ATCC). (n.d.). BT-20 (ATCC® HRB-19™). Retrieved from <https://www.atcc.org/products/htb-19>
3. Arteaga, C. L., Sliwkowski, M. X., Osborne, C. K., Perez, E. A., Puglisi, F., & Gianni, L. (2012). Treatment of HER2-positive breast cancer: current status and future perspectives. *Nature reviews Clinical oncology*, 9(1), 16-32.
4. Aulsebrook, M. L., Graham, B., Grace, M. R., & Tuck, K. L. (2018). Lanthanide complexes for luminescence-based sensing of low molecular weight analytes. *Coordination Chemistry Reviews*, 375, 191-220.
5. Baselga, J., Norton, L., Albanell, J., Kim, Y. M., Mendelsohn, J., & Arteaga, C. L. (1996). Recombinant humanized anti-HER2 antibody (Herceptin) enhances the antitumor activity of paclitaxel and doxorubicin against HER/neu overexpressing human breast cancer xenografts. *Cancer Research*, 56(13), 2759-2765.
6. Brockhoff, G., Heckel, B., Schmidt-Bruecken, E., Plander, M., Hofstaedter, F., Vollmann, A., & Diermeier, S. (2007). Differential impact of Cetuximab, Pertuzumab and Trastuzumab on BT474 and SK-BR-3 breast cancer cell proliferation. *Cell proliferation*, 40(4), 488-507.
7. Budi, H. S., Ahmad, F. N., Achmad, H., Ansari, M. J., Mikhailova, M. V., Suksatan, W., ... & Marofi, F. (2022). Human epidermal growth factor receptor 2 (HER2)-specific chimeric antigen receptor (CAR) for tumor immunotherapy; recent progress. *Stem Cell Research & Therapy*, 13(1), 40.
8. Burdall, S. E., Hanby, A. M., Lansdown, M. R., & Speirs, V. (2003). Breast cancer cell lines: friend or foe? *Breast cancer research*, 5(2), 1-7.
9. Dhritlahre RK, Saneja A. Recent advances in HER2-targeted delivery for cancer therapy. *Drug Discov Today*. 2021 May;26(5):1319-1329. doi: 10.1016/j.drudis.2020.12.014. Epub 2020 Dec 24. PMID: 33359114.

10. Eliseeva, S. V., Nguyen, T. N., Kampf, J. W., Trivedi, E. R., Pecoraro, V. L., & Petoud, S. (2022). Tuning the photophysical properties of lanthanide (iii)/zinc (ii)'encapsulated sandwich' metallacrowns emitting in the near-infrared range. *Chemical science*, *13*(10), 2919-2931.
11. Engel, R. H., Kaklamani, V. G. (2007) HER2-positive breast cancer: current and future treatment strategies, *Drugs* *67* (9) 1329–1341.
12. Faltus, T., Yuan, J., Zimmer, B., Kramer, A., Loibl, S., Kaufmann, M., & Strebhardt, K. (2004). Silencing of the HER2/neu gene by siRNA inhibits proliferation and induces apoptosis in HER2/neu-overexpressing breast cancer cells. *Neoplasia*, *6*(6), 786-795.
13. Frangioni, J. V. (2003). In vivo near-infrared fluorescence imaging. *Current opinion in chemical biology*, *7*(5), 626-634.
14. Furrer, D., Sanschagrin, F., Jacob, S., & Diorio, C. (2015). Advantages and disadvantages of technologies for HER2 testing in breast cancer specimens. *American journal of clinical pathology*, *144*(5), 686-703.
15. Gajria D, Chandarlapaty S. HER2-amplified breast cancer: mechanisms of trastuzumab resistance and novel targeted therapies. *Expert Rev Anticancer Ther*. 2011 Feb;*11*(2):263-75. doi: 10.1586/era.10.226. PMID: 21342044; PMCID: PMC3092522.
16. Hamer J, Warner E. Lifestyle modifications for patients with breast cancer to improve prognosis and optimize overall health. *CMAJ*. 2017 Feb *21*;189(7):E268-E274. doi: 10.1503/cmaj.160464. PMID: 28246240; PMCID: PMC5318212.
17. Hernot, S., van Manen, L., Debie, P., Mieog, J. S. D., & Vahrmeijer, A. L. (2019). Latest developments in molecular tracers for fluorescence image-guided cancer surgery. *The lancet oncology*, *20*(7), e354-e367.
18. Hervé-Aubert, K., Allard-Vannier, E., Joubert, N., Lakhrif, Z., Alric, C., Martin, C., ... & Chourpa, I. (2018). Impact of site-specific conjugation of ScFv to multifunctional nanomedicines using second generation maleimide. *Bioconjugate Chemistry*, *29*(5), 1553-1559.

19. Holliday, D. L., & Speirs, V. (2011). Choosing the right cell line for breast cancer research. *Breast cancer research*, *13*, 1-7.
20. Hong, G., Lee, J. C., Robinson, J. T., Raaz, U., Xie, L., Huang, N. F., ... & Dai, H. (2012). Multifunctional in vivo vascular imaging using near-infrared II fluorescence. *Nature medicine*, *18*(12), 1841-1846.
21. Hudis, C. A. (2007). Trastuzumab-mechanism of action and use in clinical practice. *New England Journal of Medicine*, *357*(1), 39-51.
22. Keereweer, S., Kerrebijn, J.D.F., van Driel, P.B.A.A. *et al.* Optical Image-guided Surgery—Where Do We Stand? *Mol Imaging Biol* **13**, 199–207 (2011). <https://doi.org/10.1007/s11307-010-0373-2>
23. Loibl, S., & Gianni, L. (2017). HER2-positive breast cancer. *The Lancet*, *389*(10087), 2415-2429.
24. Martinić, I., Eliseeva, S. V., & Petoud, S. (2017). Near-infrared emitting probes for biological imaging: Organic fluorophores, quantum dots, fluorescent proteins, lanthanide (III) complexes and nanomaterials. *Journal of Luminescence*, *189*, 19-43.
25. Martinić, I., Eliseeva, S. V., Collet, G., Luo, T. Y., Rosi, N., & Petoud, S. (2019). One Approach for Two: Toward the Creation of Near-Infrared Imaging Agents and Rapid Screening of Lanthanide (III) Ion Sensitizers Using Polystyrene Nanobeads. *ACS Applied Bio Materials*, *2*(4), 1667-1675.
26. Mezei, G., Zaleski, C. M., & Pecoraro, V. L. (2007). Structural and functional evolution of metallocrowns. *Chemical reviews*, *107*(11), 4933-5003.
27. Moelans, C. B., De Weger, R. A., Van der Wall, E., & Van Diest, P. J. (2011). Current technologies for HER2 testing in breast cancer. *Critical reviews in oncology/hematology*, *80*(3), 380-392.
28. Molina, M. A., Codony-Servat, J., Albanell, J., Rojo, F., & Arribas, J. (2001). Trastuzumab (Herceptin), a humanized anti-Her2 receptor monoclonal antibody, inhibits basal and activated Her2 ectodomain cleavage in breast cancer cells. *Cancer Research*, *61*(12), 4744-4749.

29. Nunes, J. P., Morais, M., Vassileva, V., Robinson, E., Rajkumar, V. S., Smith, M. E., & Chudasama, V. (2015). Functional native disulfide bridging enables delivery of a potent, stable and targeted antibody–drug conjugate (ADC). *Chemical Communications*, 51(53), 10624-10627.
30. Ostrowska, M., Fritsky, I. O., Gumienna-Kontecka, E., & Pavlishchuk, A. V. (2016). Metallacrown-based compounds: Applications in catalysis, luminescence, molecular magnetism, and adsorption. *Coordination Chemistry Reviews*, 327, 304-332.
31. Patel, A., Unni, N., & Peng, Y. (2020). The changing paradigm for the treatment of HER2-positive breast cancer. *Cancers*, 12(8), 2081.
32. Peng, X. X., Zhu, X. F., & Zhang, J. L. (2020). Near infrared (NIR) imaging: exploring biologically relevant chemical space for lanthanide complexes. *Journal of Inorganic*
33. Pupa, S.M.; Ligorio, F.; Cancila, V.; Franceschini, A.; Tripodo, C.; Vernieri, C.; Castagnoli, L. HER2 Signaling and Breast Cancer Stem Cells: The Bridge behind HER2-Positive Breast Cancer Aggressiveness and Therapy Refractoriness. *Cancers* **2021**, *13*, 4778. <https://doi.org/10.3390/cancers13194778>
34. Rampersad, S. N. (2012). Multiple applications of Alamar Blue as an indicator of metabolic function and cellular health in cell viability bioassays. *Sensors*, 12(9), 12347-12360.
35. Sabbatini, N., Guardigli, M., & Manet, I. (1996). Antenna effect in encapsulation complexes of lanthanide ions. *Handbook on the physics and chemistry of rare earths*, 23, 69-119.
36. Shang, L., Dong, S., & Nienhaus, G. U. (2011). Ultra-small fluorescent metal nanoclusters: synthesis and biological applications. *Nano today*, 6(4), 401-418.
37. Siegel, R.L.; Miller, K.D.; Jemal, A. Cancer statistics, 2020. *CA Cancer J. Clin.* **2020**, *70*, 7–30
38. Sliwkowski, M. X., Lofgren, J. A., Lewis, G. D., Hotaling, T. E., Fendly, B. M., & Fox, J. A. (1999). Nonclinical studies addressing the mechanism of action of trastuzumab (Herceptin). *Seminars in Oncology*, 26(4 Suppl 12), 60-70.

39. Smith, A. M., Mancini, M. C., & Nie, S. (2009). Second window for in vivo imaging. *Nature nanotechnology*, 4(11), 710-711.
40. TeachMeSurgery. (n.d.). Breast Carcinoma in Situ. TeachMeSurgery. Retrieved from <https://teachmesurgery.com/breast/malignant-disease/breast-carcinoma-in-situ/>
41. Vu, T., & Claret, F. X. (2012). Trastuzumab: updated mechanisms of action and resistance in breast cancer. *Frontiers in oncology*, 2, 62.
42. Waks AG, Winer EP. Breast Cancer Treatment: A Review. *JAMA*. 2019;321(3):288–300. doi:10.1001/jama.2018.19323
43. Wang, X., Chang, H., Xie, J., Zhao, B., Liu, B., Xu, S., ... & Huang, W. (2014). Recent developments in lanthanide-based luminescent probes. *Coordination Chemistry Reviews*, 273, 201-212.
44. WebMD. (n.d.). Breast cancer survival rates. Retrieved from <http://www.webmd.com/breast.cancer/guide/breast-cancer-survival-rates>
45. Wu, Y., Zeng, F., Zhao, Y., & Wu, S. (2021). Emerging contrast agents for multispectral optoacoustic imaging and their biomedical applications. *Chemical Society Reviews*, 50(14), 7924-7940.
46. Xi, L., & Jiang, H. (2016). Image-guided surgery using multimodality strategy and molecular probes. *Wiley Interdisciplinary Reviews: Nanomedicine and Nanobiotechnology*, 8(1), 46-60.
47. Xu, J., & Shang, L. (2018). Emerging applications of near-infrared fluorescent metal nanoclusters for biological imaging. *Chinese Chemical Letters*, 29(10), 1436-1444.7

## ABSTRACT

Breast cancer (BC) is one of the most common malignancies worldwide and a leading cause of death among women. The HER2 positive breast cancer (overexpressing HER2 receptor) represents a very aggressive subtype and constitutes 15-20% of BC cases. Here we report about the creation of new diagnostic tool based on polystyrene beads incorporating Ln-based metallocrowns that were biologically targeted in a reaction of conjugation with Trastuzumab (Trz). The bioconjugation reaction was performed under various conditions. The resulting anti-HER2 conjugated beads were tested *in vitro* in studies of affinity, cytotoxicity and proliferation. We managed to do successful bioconjugation of Trz to polystyrene beads under optimized conditions. The conjugated compound exhibited preserved binding affinity for HER2 and showed specific interactions with HER2-overexpressing cells, the conjugate did not display extensive cytotoxic effects but inhibited the proliferation of HER2-overexpressing cells. These findings suggest the potential of Trz-beads as a targeted diagnostic tool for HER2-positive breast cancer.

Key words: breast cancer, HER2 receptor, bioconjugation, polystyrene beads, metallocrown, Trastuzumab, lanthanide, near-infrared, optical imaging, nanotechnology.

## RÉSUMÉ

Le cancer du sein est l'un des cancers les plus fréquents dans le monde et l'une des principales causes de décès chez la femme. Les tumeurs HER-positive (amplification ou surexpression de du gène *HER2*) représente 15-20% des tumeurs mammaires et constitue un sous-type de cancer particulièrement agressif. Dans ce travail, nous mettons en avant la création d'un nouvel outil diagnostic basé sur l'utilisation de billes de polystyrènes contenant des macromolécules coordonnant des lanthanides luminescents et couplées à un anticorps, le Trastuzumab (Trz). La réaction de bioconjugaison a été testée dans des conditions variées pour permettre d'obtenir un rendement adéquat de couplage de billes à l'anticorps. Les billes conjuguées ont ensuite été testées pour leur affinité envers HER2, leurs effets sur la prolifération et la mort cellulaire *in vitro*. Nous avons réussi à optimiser la bioconjugaison du Trz et mis en évidence que ces composés pouvaient interagir avec les cellules HER2+. Les conjugués ne présentent pas d'effet cytotoxiques sur les cellules mais contribuent à inhiber leur prolifération. Ces résultats suggèrent le rôle potentiel des billes couplées au Trz pour la détection des cellules HER2-positive dans les cancers du sein.

Mots clés : cancer du sein, HER2, bioconjugaison, billes de polystyrène, métallacouronnes, Trastuzumab, lanthanide, proche-infrarouge, imagerie optique, nanotechnologie.